

Graphene-based semiconductor nanostructures

P B Sorokin, L A Chernozatonskii

DOI: 10.3367/UFNe.0183.201302a.0113

Contents

1. Introduction	105
2. Methods of graphene preparation	106
3. Graphene ribbons	107
3.1 Classification; 3.2 Methods of preparation; 3.3 Electronic and conducting properties; 3.4 Dependence of the electronic structure of graphene ribbons on elastic stresses; 3.5 Chemical modification of ribbons	
4. Graphane and fluorographane	115
4.1 Methods of preparation and stability of structures; 4.2 Electronic properties; 4.3 Diamanes	
5. Graphene-based electronic superlattices and waveguides	118
5.1 Chains of hydrogen atoms on graphene; 5.2 Graphene roads on graphane and fluorographane; 5.3 Graphene-ribbon-based superlattices	
6. Conclusions	120
References	120

Abstract. One of the current priorities in the physics and chemistry of graphene is the study of its semiconducting derivatives. This review summarizes the state of the art in this area of research. The structure and electronic properties of materials as such graphene ribbons, partially hydrogenated and fluorinated graphene, graphane, fluorographane, and diamane are discussed in detail.

1. Introduction

The various allotropic forms of carbon have always attracted special attention of the scientific community. Graphite and diamond, which are known from the earliest times, are widely used in daily life, and organic molecules, in which carbon atoms play the primary role, are the basis for all living things on our planet. The great variety of crystalline and molecular carbon-based structures, which manifest very different properties, is mainly related to the specific structure of the electronic shells of carbon, which allows compounds with various coordinations to form.

Since 1985, reports on new carbon-based structures were appearing regularly; the discovery of each of them invariably provokes an explosion of interest. A start to these investigations was made by the discovery of fullerenes [1], which had been predicted theoretically by various groups of authors [2, 3]. In 1991, Iijima [4] obtained images and for the first time identified structures of carbon nanotubes (CNTs), showing that the carbon in them forms a continuous hexagonal network similar to a wrapped graphite sheet. Almost simultaneously and somewhat later, films [5–9] and powders [10–11] of CNTs were obtained in macroscopic quantities. We also note that nanotubes were observed experimentally [12–17] and described theoretically in earlier works [18, 19]. It probably can be said without exaggeration that precisely from these discoveries did a new avenue in modern science — nanotechnology — originate.

Although graphite, which is one of the allotropic forms of carbon (having a structure of molecularly bound layers, with a hexagonal lattice of each layer consisting of sp^2 hybridized carbon atoms) is well known in the world, it was only in 1970–1980 that several research groups had success in obtaining a single graphite layer on pure surfaces of metallic crystals. A graphite monolayer was first successfully synthesized on the surface of nickel by scientists in Blakely's research group [20–23]; later, such a monolayer was grown on crystals of lanthanum hexaboride [24], platinum [25], iridium and rhenium (in Tontegode's group [26–29]), and titanium carbide [30], and, in 2003, on the surface of silicon carbide [31]. In 1961, Boem et al. [32] reported the preparation of an isolated graphite layer as an intermediate phase in synthesizing graphene oxide. However, only the work of the group of Geim and Novoselov (Russia–Great Britain) became truly revolutionary, in which a graphite monolayer — a graphene sheet — was obtained in a free-standing state (Fig. 1) [33–35]. In 2010, Andrei Geim and Konstantin Novoselov were awarded a Nobel Prize in physics

P B Sorokin Technological Institute for Superhard and Novel Carbon Materials,
ul. Tsentral'naya 7a, 142190 Troitsk, Moscow, Russian Federation;
Emanuel Institute of Biochemical Physics, Russian Academy of Sciences,
ul. Kosygina 4, 119334 Moscow, Russian Federation
L A Chernozatonskii Emanuel Institute of Biochemical Physics,
Russian Academy of Sciences,
ul. Kosygina 4, 119334 Moscow, Russian Federation
Tel. +7 (495) 939 71 72
Fax +7 (499) 135 41 01
E-mail: cherno@sky.chph.ras.ru

Received 30 January 2012

Uspekhi Fizicheskikh Nauk **183** (2) 113–132 (2013)

DOI: 10.3367/UFNr.0183.201302a.0113

Translated by S N Gorin; edited by A M Semikhatov

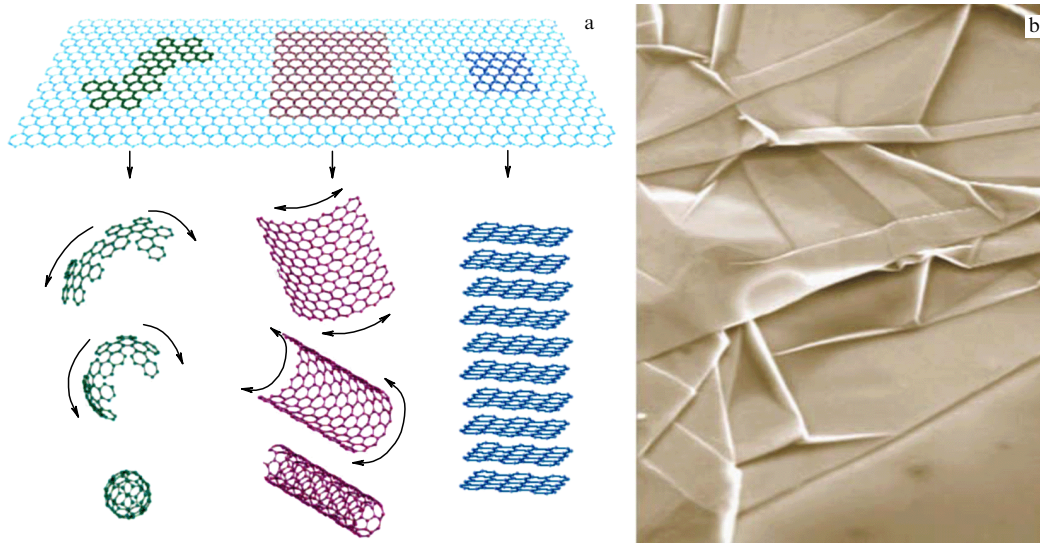


Figure 1. (a) Graphene as the basis for graphite-like materials: fullerene, nanotubes, and graphite [62]; and (b) a photo of graphene [36].

for the discovery and investigation of the extraordinary properties of graphene.¹

Graphene can be regarded as the base for the preparation of any graphite-like materials because it can be ‘wrapped’ into a molecule of fullerene or into a carbon nanotube, and the graphite crystal in fact consists of graphene sheets (Fig. 1a). We note that the situation with the investigations of graphene is unique in that its theoretical study started already in the middle of the 20th century [37–39], because graphene frequently served as a model in the investigations of graphite-like materials, with the interlayer interaction in graphite ignored.

The term ‘graphene’ was introduced by the International Union of Pure and Applied Chemistry (IUPAC) in 1994 [40], i.e., significantly earlier than 2004 (when graphene was obtained [33–35]) in view of the necessity of describing structures consisting of isolated graphite layers; however, the possibility of the existence of isolated extended two-dimensional carbon layers was out of the question at that time, in particular, because it was then commonly accepted that such purely two-dimensional objects should be unstable [41].

Graphene has a number of interesting properties (these are described in much detail in reviews [42–53]) which allow considering it a potential material for nanoelectronics. However, its fundamental feature — its half-metallic conductivity — restricts its application directly in semiconducting electronics devices. One of the main problems of the modern physics of this material is the creation of a dielectric gap in its electronic spectrum. For this, a number of various approaches have been developed, such as functionalization, the introduction of defects into the graphene structure, and the cutting of isolated ribbons from graphene.

In this review, we try to systematize the vast body of available data on graphene-based structures having semiconducting properties, which can be caused by quite various factors, such as defects in their structure, unusual types of bonding between the atoms, or surface and quantum size effects.

2. Methods of graphene preparation

The methods of graphene preparation have been described in detail in Refs [50–55], and in this review we therefore discuss only some pioneering and fundamental results. In the work from which the ‘graphene rush’ began [33, 34], isolated graphene sheets were obtained by the method of so-called micromechanical cleavage or the scotch-tape technique: an adhesive tape was glued on two sides to a crystal of highly oriented graphite and was then torn off, leaving microscopic pieces of graphite on it. Then a new piece of tape was glued to these pieces and the tearing-off procedure was repeated (see the movie in [56]). After several repetitions, atomic graphite layers — graphene — could be revealed. This process can easily be understood from the physical standpoint, because graphite represents a stack of graphene sheets attached to one another by van der Waals bonds. Upon being torn off, these bonds become broken, and the material cleaves.

Generally speaking, this simple but efficient scotch-tape technique can be applied not only to graphite but also to other layered materials [33]. The use of this technique allows obtaining monolayers up to 100 μm in size. A similar approach was also used by other research groups [57–61], but they obtained only samples with thicknesses from 20 to 100 graphite layers. The problem is that the graphene structures remaining in the substrate are formed only rarely and are usually hidden between multilayer graphite crystals, and even the application of the whole arsenal of modern methods of investigation by no means always guarantees the detection of graphene monolayers.

An important factor that ensured the success proved to be one specific feature of graphene: it becomes visible in an optical microscope when placed onto a substrate of silicon dioxide of a certain exact definite thickness, which creates an interference effect that permits reliably distinguishing between the substrate and the overlying monolayer structure. A deviation in the substrate thickness by only 5% (315 nm instead of 300 nm) makes the graphene on such a substrate completely invisible [62]. However, the use of various narrow-band filters allows obtaining clear images of graphene on substrates of different thicknesses [63].

¹ A translation of the Nobel lectures into Russian can be found in [49, 276].

One more efficient method for the detection of graphene samples is Raman scattering. The spectra of monolayer and multilayer graphene sheets were analyzed in a number of studies [64–66]. It has been established that the number of layers in the structure can be uniquely determined from the shape and intensity of the peaks. In Ref. [66–69], based on the information on the positions and intensity of peaks in the spectra, an image of graphene was constructed. The method of Raman scattering also allows identifying the type of the edges of graphene samples [66, 70], which is especially important for the determination of the type of graphene ribbons (see Section 3.1).

Earlier attempts to prepare graphene were based on the methods of chemical exfoliation. Graphite was subjected to intercalation by some species to increase the spacing between neighboring sheets [71]. However, the introduction of large-size molecules in some cases led to a structure in which separate graphite sheets were introduced into a three-dimensional matrix.

The intercalation of graphite can be used as a method of obtaining graphene [72–74], but this way is of limited interest because of its uncontrollable character.

Monolayers and bilayers of graphene can be grown epitaxially using the method of chemical vapor deposition from hydrocarbons on a metal surface. A two-dimensional graphite film can be formed on the surface of crystal faces of some metals and compounds, e.g., TaC [75], Pt [25], Ni [20–23, 76, 77], Re [27, 28], Ir [226, 228], LaB₆ [24], TiC [30], Au [79], Cu [80–85], Ru [86–88], Co [89, 90], Rh [91, 92], Fe [93], Pd [89], and Re [27, 78]. We make a special note of Ref. [85], in which the authors reported on the preparation of a 30-inch graphene film. The technology of the production of the material is as follows: graphene is grown on copper foil sheets by the method of chemical vapor deposition and is then rolled on a polymer. Copper is removed by etching, after which graphene is applied onto a required substrate by passing it between rolls with simultaneous heating (~90–120 °C). The structure obtained consists predominantly of monolayer graphene with two-layer and multilayer islands. The material has characteristics (90% optical transmittance, sheet resistance up to 30 Ω per unit area) that exceed those of the known analogs (such as films of indium tin oxide or carbon nanotubes), which makes them promising for applications in modern electronics. In [85], the authors also successfully used the thus-obtained graphene film as the base for a touch-screen panel.

Any organic material can in fact be used as the source of carbon. The researchers of Tour's group [84] reported the preparation of high-quality graphene on a copper substrate from food, waste, and even insects. The Raman scattering spectra taken from such a film show a moderate D peak, which indicates a high quality of the graphene structure.

Pioneering study [34] on graphene led to an explosive development of two-dimensional nanostructures of other chemical compositions. Two-dimensional structures of compounds such as NbSe₂, Bi₂Sr₂CaCu₂O_x, MoS₂ [34], BN [34, 94–97], Bi₂Te₃ [98], MoS₂ [99, 100], ZnO [101, 102], Cu₂O [103], SiC [104], silicon covered by an oxygen layer containing magnesium (with the total structure formula Si_{7.0}Mg_{1.3}O_{7.5}) [105], and quartz glass SiO₂ [106] have been obtained by various methods experimentally, whereas structures on the basis of boron [107], germanium [108–111], CN, SiN [111], GaN [112], NbSe₂ [108], and SiO₂ [113] have been suggested and studied theoretically.

3. Graphene ribbons

Estimates show that a graphene nanoribbon (GNR), just like a monolayer CNT, due to the quantum size effect arising because of its nanosize width, can have an energy gap whose width is sufficient for the use of GNRs in electronics. Long before the experimental preparation of GNRs, Wakabayashi et al. [114, 115] and Nakada et al. [116] studied the electronic structure and magnetic properties of graphene nanoribbons in detail. A theoretical analysis of these properties was carried out, along with an intense study of CNTs; as a result, naturally, both similarities and differences in the characteristics of these objects were established.

3.1 Classification

Some similarity between carbon nanotubes and graphene ribbons is emphasized by analogies in their classification [116]. We recall that the structure of nanotubes is described by two integer numbers (n, m) indicating the coordinates of the hexagon that, as a result of wrapping the graphene plane, must coincide with the hexagon located at the origin. Monolayer CNTs are divided into subtypes of the 'armchair' type (n, n), 'zigzag' type ($n, 0$), and chiral (n, m), where $n > m$. The structures of the nanotubes corresponding to the armchair and zigzag configurations are shown in Fig. 2a.

Graphene ribbons are also divided into 'armchair' and 'zigzag' subtypes, but they are assigned to a particular type depending on the shape of their edges rather than their sections, in contrast to CNTs. The most common types of nanoribbons—zigzag (ZGNRs) and armchair (AGNRs)—are shown in Figs 3b and 3c. These have only one index, which is proportional to the ribbon width. In the case of a zigzag ribbon, the index is equal to the number of atoms, and in the case of an armchair ribbon, it is the number of dimers C₂ that are located in the cross section of the ribbon.

The expression for the ribbon width is [114]

$$W = \begin{cases} \left(\frac{3}{2}N - 1\right)a \equiv W_z, \\ \frac{\sqrt{3}}{2}(N - 1)a \equiv W_a, \end{cases} \quad (1)$$

where W_z and W_a are the widths of the zigzag and armchair ribbons, a is the length of the carbon–carbon bond in graphene (1.42 Å), and N is the index of the ribbon.

We note that ribbons with edges passivated by hydrogen atoms are usually studied. In this case, in spite of an increase in the ribbon width, the classification remains the same: only the number of carbon atoms in the ribbon cross section is determined. Because the atoms that are located at the edges of the ribbon have uncompensated electrons, which tend to become bound with the atoms of the surroundings, the passivation leads to only a slight change in the electronic properties of the nanoribbons (see Section 3.3).

3.2 Methods of preparation

After the preparation of graphene, interest naturally arose in the study of graphene ribbons. There are grounds to believe that precisely the ribbon structures will be the base for the nanoelectronic circuits in the future, i.e., will play the role of nanodiodes and nanotransistors in them, as well as of the elements of spintronics. We note that the semiconducting properties of GNRs manifest themselves only until the ribbon width is less than ~20 nm and that the energy gap of ribbons

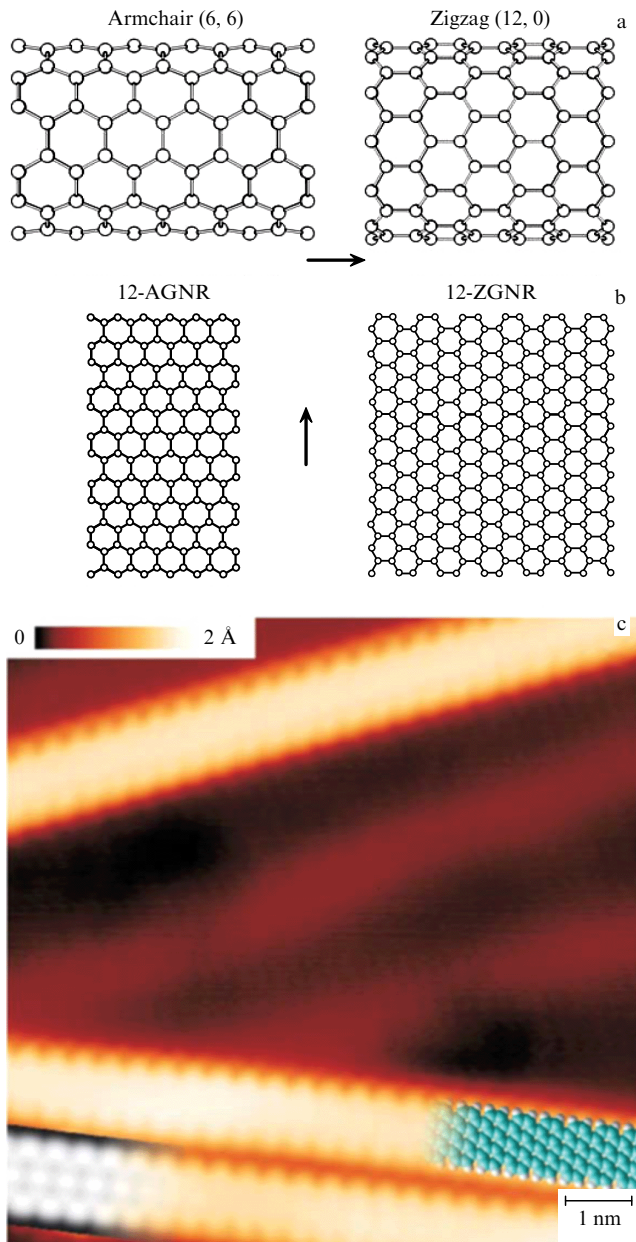


Figure 2. Comparison of the notation for monolayer nanotubes and ribbons: (a) on the left, an armchair CNT with indices (6, 6); on the right, a zigzag CNT with indices (12, 0); (b) on the left, an armchair graphene nanoribbon with the index 12 (12-AGNR); on the right, a zigzag-type ribbon, index 12 (12-ZGNR). The arrows indicate the periodic direction of the structures. (c) Images of graphene ribbons obtained experimentally [146] using high-resolution scanning tunneling microscopy.

decreases proportionally to their width (see Section 3.3). This is the main obstacle in the investigations and applications of GNRs.

As the main method of obtaining GNRs, electron lithography is most efficient, in which the graphene can be cut into isolated parts by an electron beam. This method was used in Avouris's [117] and Kim's [118] research groups; graphene coated with hydrogen silsesquioxane was exposed to oxygen plasma to remove graphene parts uncovered with the coating. As a result, ribbons 10–100 nm wide and 1–2 μm long were obtained. The advantage of this method is in the possibility of controlling the ribbon width; its disadvantage is in the complexity of controlling the shape of ribbon edges, which substantially determine the electronic properties of the ribbons. Apart from electron lithography, the method of scanning tunneling microscopy (STM) at a high voltage can be used [119]. This method (with a voltage of 2.4 V between the STM tip and the graphene) has allowed preparing armchair-type ribbons of a minimum width (3.5 nm) with a defect-free structure.

One more possibility of obtaining graphene ribbons by the method of nanolithography was described in [120, 121]. Graphene coated with a film with holes arranged in a hexagonal order was exposed to oxygen plasma; as a result, a hexagonal network of graphene ribbons with more than 7 nm in width was formed.

It is reasonable to use another promising nanomaterial — nanowires — as a base for growing GNRs because the nanometer transverse size of these objects should determine the width of the graphene ribbons. In [122], silicon nanowires were used to protect graphene from the action of oxygen plasma. This method allowed obtaining GNRs with widths starting at 6 nm.

For the production of graphene ribbons, the method of electrostatic transfer can also be used [123]. This method is based on the fact that on the surface of well-cleaned, highly oriented graphite, there are always pieces of graphene consisting of several atomic layers. They can be relatively easily separated from the graphite surface using the electrostatic field of the tip of a scanning tunneling microscope. Varying the applied voltage, nanographenes consisting of different numbers of atomic layers can be taken off. Using this method, ribbons measuring 50 nm in width and more than 500 nm in length have been obtained. But the width and shape of the ribbons obtained, which are important for specifying their definite electronic properties, are difficult to control. Therefore, the ribbons should additionally be treated by an electron beam.

One of the most important problems in modern nanotechnology is the development of a method that would allow

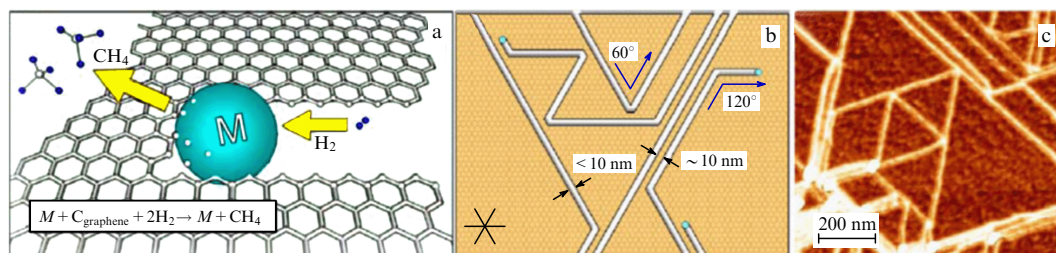
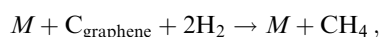


Figure 3. Schematic of (a) the process of etching and (b) the result of etching of graphene with metallic nanoparticles; (c) image of graphene after etching (atomic force microscopy [126]).

fabricating ribbons with transverse sizes of the order of a few nanometers with smooth edges. The method developed in Dai's group [124] satisfies at least the first of the above-mentioned requirements: the ribbons were less than 10 nm wide. The experiment consisted of several stages: first, graphite was delaminated upon fast (60 s) heating to 1000 °C in a gas atmosphere consisting of 3% hydrogen in argon. Then the obtained species was dispersed in a solution of 1,2-dichloroethane with poly(m-phenylenevinylene-co-2,5-dioxy-p-phenylenevinylene) (PmPV) under the effect of ultrasound (30 min) to obtain a homogeneous suspension. The larger particles were removed by centrifugation; among the remaining particles, graphene ribbons with a width from 1 to 10 nm were revealed using atomic force microscopy.

In Refs [125–1227], a method of etching graphene was developed using metal nanoclusters (Ni [125, 1226], Fe [127]), which was used as a chemical analog of scissors for cutting graphene in strictly defined directions specified by the crystallography of the sheet. The 'cutting' of graphene can be described by the reaction



where $M = \text{Fe, Ni}$, and C_{graphene} are the carbon atoms of graphene (Fig. 3a). At a high temperature (~ 1000 °C), metal clusters ~ 10 nm in size diffuse through the graphene, 'cutting' it. In this way, ribbons with a width of less than 50 nm and a length of about 1 μm were obtained (Fig. 3b). An image of graphene after etching is shown in Fig. 3c. An especially interesting feature is the selectivity of the directions of graphene etching; it turned out that the metal particles etch the graphene at angles of 60° and 120°, corresponding to the symmetry of the unit cell of graphene. We note that in the etching of multilayer graphene or graphite [126], the spread of the etching angles increases; the angles equal to 30°, 60°, 90°, 120°, and 150° appear. A theoretical analysis [125] has shown that because the energies required to remove one carbon atom from the edges of zigzag and armchair configurations differ substantially (1.852 and 0.518 eV, respectively), only zigzag ribbons should be obtained as a result of etching. This assumption was confirmed experimentally in [126, 128].

The process of etching can also occur in the absence of metal clusters. In [129], Wang and Dai have studied a method for etching graphene by oxidation of its edges. As the initial material, they used wide ribbons (20–30 nm wide) obtained by the method of electron lithography. This technique allows preparing ribbons less than 10 nm wide; in addition, branched graphene ribbons — analogs of multiterminal carbon nanotubes — can thus be obtained.

Nemes-Incze et al. [130] used a two-stage technique of graphene etching. At the first stage, graphene was placed in an oxygen–nitrogen atmosphere at 500 °C, which led to the appearance of oval holes in the graphene structure. Then the obtained defect structure was exposed to an argon flow at 700 °C. Under the effect of the active medium, the holes began expanding such that the armchair edges were etched faster than the zigzag edges (in full agreement with the theoretical estimates [125]), acquiring a hexagonal symmetry as a result. This technique allowed obtaining ribbons with a width of more than 35 nm.

Yang et al. [131] used a similar principle, but graphene was placed in hydrogen plasma at 500 °C. This procedure led to the appearance of holes of hexagonal shape, as in [130]. Then, using electron lithography and oxygen plasma at room

temperature, graphene ribbons about 120 nm wide were obtained. The subsequent treatment in hydrogen plasma was used to narrow the ribbons even more, such that their width became less than 20 nm. The method of local electrooxidation with the help of atomic force microscopy was used in [132], which allowed obtaining graphene ribbons ~ 25 nm wide.

Apart from graphene, nanotubes are a potentially suitable base for the production of GNRs. The cutting ('unzipping') of nanotubes should permit obtaining ribbons of high quality and long length. The process of etching CNTs with clusters of nickel and cobalt deposited on their surface [133] occurs at 850 °C in a weak flow of H_2 –Ar; as a result, nanotubes completely or partly cut along the axis can be obtained. Large metal clusters (~ 40 nm) can cut deep grooves in the tube structure, opening multilayer CNTs [133]. We note that the partly cut nanotubes also represent independent interesting objects, in which, according to theoretical predictions, a significant magnetoresistance can be observed [134]. In addition, these structures can be regarded as CNT–GNR–CNT superlattices (see Section 5.3).

Graphene ribbons can be obtained from nanotubes not only by using catalysts. From multilayer carbon nanotubes (MCNTs), stacks of graphene ribbons can be obtained by heating in a vacuum to 1800 °C [135]. A similar transformation was achieved in [136] by annealing an MCNT sample at high pressure (5.5 GPa), and in [137] by intercalating an MCNT sample by lithium in liquid ammonia with subsequent exfoliation (at a temperature of 1000 K).

In Tour's group, a method was used in which the nanotubes were cut along the axis by oxidation with potassium permanganate in the presence of concentrated sulfuric acid [138]. The efficiency of this method was found to be very high; the yield of ribbons was almost 100%, but their quality turned out to be low. In another work by the same group [139], the nanotubes were oxidized at 60 °C in the presence of a mixture of a compound and an acid (H_2SO_4 – $KMnO_4$, $C_2HF_3O_2$, or H_3PO_4). The ribbons obtained demonstrated excellent characteristics (high quality of the atomic structure and good conductivity). In the same research group, a method was developed for obtaining GNRs under the action of potassium vapors [140].

Talyzin et al. [141] have demonstrated that graphene sheets can be produced by hydrogenating carbon nanotubes. It has been shown that the action of hydrogen at 400–550 °C can lead to the unzipping of a CNT and the formation of graphene ribbons with hydrogen atoms attached to their edges. In Dai's research group [142], another method was used; carbon nanotubes placed in a solution of 1,2-dichloroethane with PmPV polymer were exposed to oxygen, which, reacting with defects in the CNT, produced holes in its surface. The subsequent action of ultrasound increased the holes and broke the structure into very narrow graphene ribbons (~ 1 nm wide) with highly smooth edges [143].

The same research group developed a physicochemical method for obtaining GNRs from MCNTs [144, 145], when the part opened along the nanotube, which was in a polymethylmethacrylate film, was cut out using argon plasma. Depending on the time of etching, a monolayer or multilayer graphene ribbon is obtained.

An interesting method was suggested in Ref. [146], where ultranarrow graphene armchair ribbons (7-AGNR) were produced by coupling 10,10'-dibromo-9,9'-bianthryl monomers. At the first stage, dehalogenation of the molecules was

performed, after which they were connected into a linear polymer chain, which after cyclodehydrogenation were transformed into an ultranarrow graphene ribbon with ideal armchair edges (Fig. 2a).

Chuvilin et al. [147] obtained ultranarrow graphene ribbons, but already with zigzag edges (4-ZGNR) inside ‘pods’ consisting of carbon nanotubes with fullerenes inside them, with attached organic groups and sulfur atoms. The action of an electron beam or high temperature transforms the fullerenes into graphene ribbons. The edges of the GNRs obtained were passivated by sulfur; precisely the presence of sulfur, in the opinion of the authors, plays the key role in the success of the synthesis of the material, because it makes the ribbons energetically more favorable structures than the initial material. The same authors have obtained graphene ribbons from tetrathiafulvalene ($C_6H_4S_4$) placed inside a carbon nanotube. The complexity of the application of this technique is in the difficulty of the subsequent extraction of the GNRs from the nanotubes. Talyzin et al. [148] used a similar method in which coronen and perylene were used as the source of carbon. As a result of heating, these molecules were transformed into GNRs 0.7 nm wide.

As was noted by the authors of [149], the thinnest possible graphene ribbons — with a width of only one benzene ring, i.e., hexaphenyl (armchair ribbon) [150] and hexacene (zigzag ribbon) [151] — were obtained and studied 50 years ago. In Ref. [152], bundles of one-dimensional graphite polymers whose structure is similar to that of graphene ribbons were studied experimentally.

3.3 Electronic and conducting properties

To describe the electronic properties of graphene ribbons, it is most suitable to use the tight-binding approximation for the π electron system [115, 116]. This model describes the main features of electronic characteristics of fullerenes, carbon nanotubes, and other structures based on graphene.

The Hamiltonian of this model is written as [153]

$$H = \sum_{\langle i,j \rangle} t_{ij} c_i^+ c_j, \quad (2)$$

where c_i^+ is the operator of electron creation in a state i , c_j is the operator of electron annihilation in a state j , and t_{ij} is the overlap integral (equal to ~ 3.0 eV for graphene). The summation is performed over nearest neighbors.

We consider the energy band structure of π electrons of graphene [37]. To diagonalize the Hamiltonian, we use a basis constructed from a two-component spinor $c_k^+ = (c_{Ak}^+, c_{Bk}^+)$ with a Fourier transform ($c_{i \in A}^+, c_{i \in B}^+$). Let \mathbf{a}_1 , \mathbf{a}_2 , and \mathbf{a}_3 be the vectors of displacements from a state A to the states of three nearest neighbors B defined such that the product $\hat{z}[\mathbf{a}_1 \mathbf{a}_2]$ is positive (Fig. 4a) (here, \hat{z} is the vector that is perpendicular to the graphite-sheet plane). Hamiltonian (2) can then be written as

$$H = \sum_k c_k^+ H_k c_k, \quad (3)$$

where

$$H_k = -t \sum_{i=1}^3 (\cos(\mathbf{k} \mathbf{a}_i) \hat{\sigma}_x + \sin(\mathbf{k} \mathbf{a}_i) \hat{\sigma}_y)$$

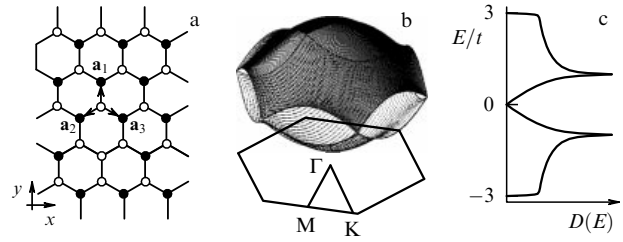


Figure 4. (a) Single layer of a graphite structure (graphene). Black dots, atoms of sublattice A; white dots, atoms of sublattice B. (b) Energy band structure for π electrons, $E(k_x, k_y)$, and the first Brillouin zone with the characteristic points (Γ , K, M). (c) Density of electron states $D(E)$ of graphene [153].

and $\hat{\sigma} = (\hat{\sigma}_x, \hat{\sigma}_y, \hat{\sigma}_z)$ are the Pauli matrices. The energy spectrum of such a Hamiltonian is

$$E_k^\pm = \pm t \left| \sum_{i=1}^3 \exp(i \mathbf{k} \mathbf{a}_i) \right|.$$

Because one carbon atom has one π electron on average, only the E_k^- band is completely filled (i.e., it is the valence band), and the E_k^+ band is the conduction band.

Figure 4b demonstrates the dispersion of energy states of the π bands in the first Brillouin zone (BZ); Fig. 4c shows the density of electron states calculated using this method.

Near the center of the Brillouin zone (the Γ point), the energies of holes in the valence band and of electrons in the conduction band have quadratic dependences on k_x and k_y . The M point is a saddle point; the density of electron states diverges logarithmically at this point. Near the K point, the energy depends on the wave vector linearly,

$$E_k^\pm = \frac{\pm 3ta|\mathbf{k}|}{2}, \quad a \equiv |\mathbf{a}_i| (i = 1, 2, 3), \quad (4)$$

just as the density of electron states does.

The graphene surface that is ‘cut’ into separate strips along the armchair or zigzag direction represents a set of GNRs of different types whose energy band structures can be obtained using the above-described formalism. In this case, we assume that the spectrum of GNRs is determined as the lines of intersection of the surface $E(k_x, k_y)$ by the planes of the allowed values of the wave vector Q perpendicular to the ribbon; $Q = 2\pi n/W$ ($n = 1, \dots$) for standing vibrations across the ribbon width W , i.e., the period of the graphene superlattice formed of like ribbons. The energy band structures of armchair and zigzag ribbons of different widths calculated by this method are given in Fig. 5.

We consider the specific features of the electronic spectrum of ribbons of both types. In the case of armchair GNRs, the bottom of the conduction band and the top of the valence band are in the center of the Brillouin zone ($k = 0$). The conductivity of these ribbons can be different depending on their index; it can be either semiconducting ($N = 3m$, $N = 3m + 1$, Figs 5a, 5c) or semimetallic ($N = 3m + 2$, Fig. 5b).

This can easily be understood from the pattern of the energy-band structure of graphene $E(k)$ (Fig. 4b), which has only two equivalent points of intersection of the cones of the valence band and the conduction band in the Brillouin zone (K and K') [154]. If the allowed value of the wave vector Q determined by the width and, consequently, by the index of

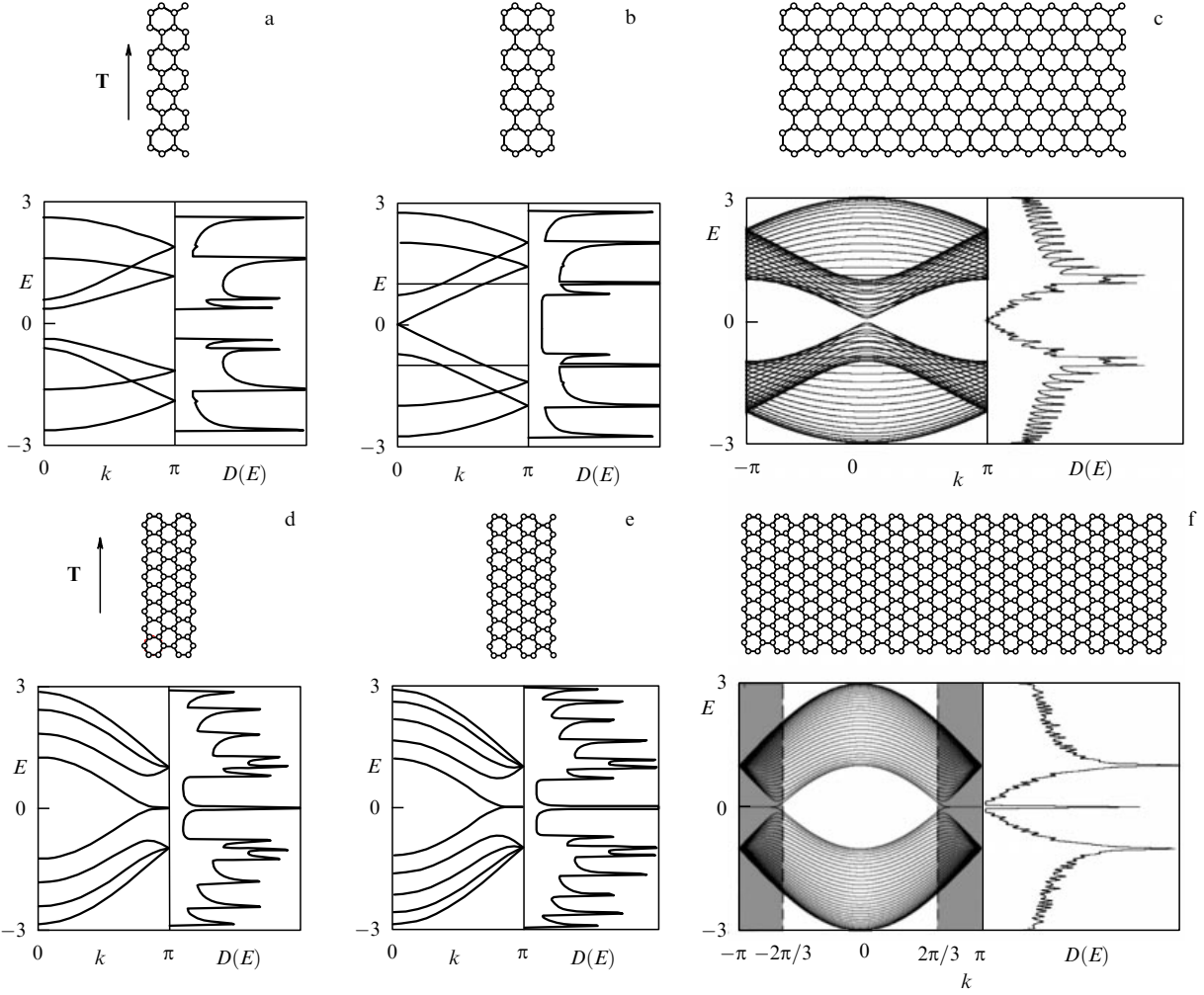


Figure 5. Atomic structure, the energy band structure $E(k)$, and the density of states $D(E)$ of armchair ribbons [(a) 4-AGNR; (b) 5-AGNR; (c) 30-AGNR] and zigzag ribbons [(d) 4-ZGNR; (e) 5-ZGNR; (f) 30-ZGNR]. In the last energy band structure, the limiting region of the existence of bands of edge states with a zero curvature is highlighted [153]. \mathbf{T} is the translation vector of the ribbons.

the GNR, coincides with the K or K' point, then an intersection of the valence band and conduction band also exists in the band structure of the graphene ribbon, and the GNR therefore manifests semimetallic properties; in the other case (where Q does not coincide with the K or K' points), it has semiconducting properties.

The zigzag ribbons have an energy band structure different from that of the armchair ribbons (Figs 5d–5f). It follows that the bottom of the conduction band and the top of the valence band of the two branches of eigenvalues $E(k)$ are always twofold degenerate at $k = \pi$. As the width of the ribbons increases, their curvature and the region of degeneracy increase in the range $2\pi/3 \leq |k| \leq \pi$. The electronic states of these branches at the Fermi level are characterized by localized states near the zigzag edge of the ribbon [115, 116]. We also note that the first report on the specific features of the electronic structure of a zigzag ribbon appeared in Ref. [155], where, using quantum mechanical calculations, Kobayashi analyzed the density of electron states of the edge of graphite that was simulated by a stack of zigzag graphene ribbons.

A significant effect of the ribbon edge on the electronic structure of graphene was demonstrated in recent experimental work [156]. The authors of [156] used scanning transmission electron microscopy and an analysis of the fine structure of spectra of absorption of electrons by separate

atoms to study the electronic properties of the graphene edge and, among other things, demonstrated the existence of a transition region ~ 1.5 nm wide that is subject to the influence of edge effects.

We next consider the behavior of the energy gap at the Γ point in the case of armchair ribbons. The Hamiltonian of an armchair ribbon can be written as

$$H = -t \sum_{j=1}^N \left(\sum_{\mu=1}^2 (a_{j,\mu}^+ a_{j+1,\mu} + \text{c.c.}) + a_{j,1}^+ a_{j,2} + \text{c.c.} \right). \quad (5)$$

The states with subscripts $(j, 1)$ and $(j, 2)$ correspond to the states $jA(B)$ and $jB(A)$, where j is an even (odd) number, and c.c. is the complex conjugate. The eigenvalues are equal to

$$\varepsilon^\pm = -2t \cos \left(\frac{n\pi}{N+1} \right) \pm t, \quad n = 1, 2, \dots, N,$$

and the corresponding eigenfunctions are

$$\Psi_{j\mu} = (\mp 1)^{\mu+1} B \sin \left(\frac{nj\pi}{N+1} \right),$$

where $\Psi_{j\mu}$ is the wave function of the state (j, μ) and B is a normalization factor. The system is ‘metallic’ if $N = 3m + 2$, because ε^+ and ε^- are respectively equal to zero at $n = m + 1$

and $n = 2m + 2$. Therefore, the width E_g^N of the bandgap of an armchair ribbon with an index N can be written as

$$E_g^N = \begin{cases} 2 \left(2t \cos \left(\frac{m}{3m+1} \pi \right) - t \right), & N = 3m, \\ 2 \left(2t \cos \left(\frac{m+1}{3m+2} \pi \right) - t \right), & N = 3m+1, \\ 0, & N = 3m+2. \end{cases} \quad (6)$$

Expressing the number N as a function of the ribbon width [Eqn (1)] and expanding in a Taylor series under the condition that $1/W_a \ll 1$, we obtain the following $E_g^N(W_a)$ dependence:

$$E_g^N \approx t \begin{cases} \frac{\pi}{W_a + \sqrt{3}/2}, & N = 3m, \\ \frac{\pi}{W_a}, & N = 3m+1, \\ 0, & N = 3m+2. \end{cases} \quad (7)$$

Here, the quantity W_a is given in units of the lattice parameter a . Hence, the bandgap width of armchair ribbons is inversely proportional to the ribbon width (Fig. 6).

Early calculations of the electronic properties of graphene ribbons performed in the tight-binding approximation qualitatively predicted the behavior of the bandgaps of graphene-based nanotubes and nanoribbons. Using this method, the authors of the pioneering work [157, 158] also predicted the dependence of the bandgap of carbon nanotubes on the mode of their folding, which was later confirmed experimentally. The same mathematical tool was used in Refs [115, 116] for the development of the theory of graphene ribbons, which is described in this section. However, the tight-binding approximation does not take the geometrical features of real structures into account, which sometimes noticeably change the electronic properties of the systems (for example, it was revealed experimentally that carbon nanotubes of a small diameter, whose semimetallic band structure was predicted using this method, exhibit semiconducting properties because of the deformation of their atomic geometry due to large curvature [159]).

According to the predictions of the tight-binding method [116], zigzag ribbons should reveal metallic properties; each third armchair ribbon should also be metallic, with a zero gap

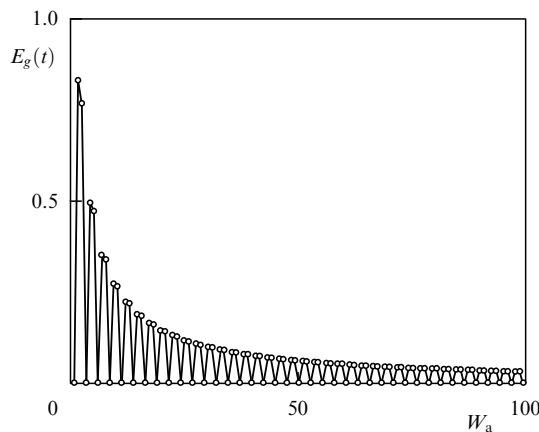


Figure 6. The energy gap width (in overlap-integral units) of an armchair ribbon as a function of the ribbon width (in bond-length a units) [153].

in the electronic spectrum. In the work by the research groups of Cohen [160] and Scuseria [161], it was shown that this statement does not correspond to reality. The results of first-principle calculations performed using the density-functional theory (DFT-LDA [160], DFT-PBE and DFT-HSE [161], DFT-GW [162]) have shown that ribbons with the indices $3m + 2$ are also semiconductors, although with a significantly narrower bandgap (less than 0.5 eV [160, 161]) than in the case of ribbons with other indices.

In the case of zigzag ribbons, the analytic results have been corrected by more exactly taking the boundary conditions into account. In Refs [160, 163], the analysis of zigzag graphene ribbons has shown that such ribbons should also exhibit semiconducting properties but with a narrower bandgap (less than 0.4 eV [160]). This conclusion was obtained taking the spin component of the zigzag GNR electrons into account. It has been found that the ground state of a zigzag GNR is antiferromagnetic [160, 164, 165] when the spin-up and spin-down states belong to the atoms of different sublattices of the graphene.

This effect leads to the loss of the mirror symmetry of the ribbon relative to its symmetry plane and to the appearance of a bandgap [160]. Therefore, this structure can be considered a spin analog of the lattice of h-BN, in which the bandgap is formed because of the difference between the ionic potentials of boron and nitrogen located in different sublattices of the compound [166]. In a later study [167], it was suggested that a zigzag ribbon can be transformed from a semiconducting into a semimetallic state by the application of a transverse electric field whose magnitude depends on the ribbon width; in particular, $E_{cr} = 0.045 \text{ V \AA}^{-1}$ for 32-ZGNR and 0.1 V \AA^{-1} for 16-ZGNR. Later, this magnitude was corrected in [168] in DFT-B3LYP calculations, where it was shown that the critical value of the field should be approximately two times greater, because the DFT-LDA approximation systematically underestimates the bandgap of graphene ribbons.

The results presented, just as the results in Refs [169, 170], where nonzero bandgaps were predicted in ribbons of finite length, permit stating that zigzag and armchair graphene ribbons should reveal only semiconducting properties, at least in the absence of extremely high external electric fields.

Ribbons with mixed-type edges, according to the predictions in [161], should exhibit a more complex behavior, depending on the width and shape of the edges (Fig. 7). It follows that mixed ribbons can already reveal metallic properties at a width of more than 1 nm.

It is of interest to compare the above predictions with available experimental results; the widths of the bandgaps for ribbons of different widths and different types of edges were estimated, e.g., in [117–120, 124, 171]. In [120], ribbons $\sim 4 \text{ nm}$ wide with a bandgap equal to 0.4 V were obtained; in [119], for ribbons with widths ~ 2.5 and $\sim 10 \text{ nm}$, the respective E_g values 0.5 and 0.18 eV were obtained. The authors of [171] have shown, using tunneling microscopy, that GNRs with a larger fraction of zigzag edges have a smaller energy gap than those of the same width with predominantly armchair edges; the dependence of their bandgaps on the ribbon width agrees with previously performed calculations [160].

Ribbons with edges of mixed types were studied in [172]. The values of the bandgap widths (from 0.05 to 0.02 eV obtained for ribbons with widths from 8 to 20 nm) proved to be smaller than in other studies, which, on the whole, agrees with the predictions made by the research group of Scuseria

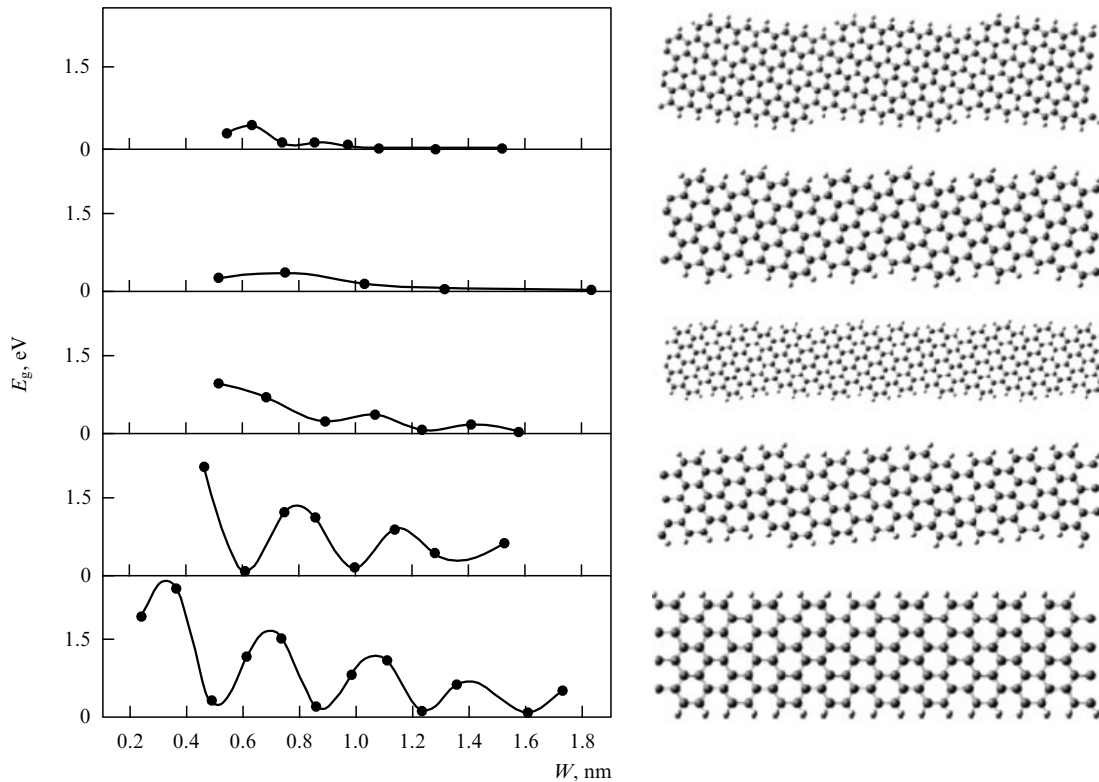


Figure 7. Dependence of the energy-gap width of graphene ribbons with mixed-type edges on the ribbon width. Calculated by the DFT-HSE method [161].

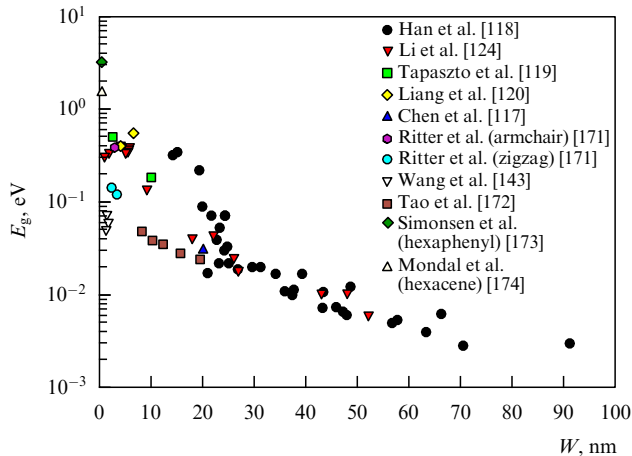


Figure 8. Experimental values of the width of the energy gaps of graphene ribbons of nanometer widths.

[161] concerning ribbons with mixed edges. The conductivity of narrow (~ 1 nm) ribbons with highly smooth edges was measured in [143]; the values of the width of their bandgaps proved to be smaller than in previous studies [119, 124, 171].

The results of all known experimental works are summarized in a common graph in Fig. 8. Because of the low resolution of the microscopes that were used, the shapes of the edges have not been determined clearly (except for [171]), and therefore the points in this figure can belong to armchair, zigzag, or mixed-type ribbons.

We note that the narrowest of all possible ribbons, hexaphenyl (armchair ribbon) and hexacene (zigzag ribbon)

(see Section 3.2), exhibit the largest bandgaps for the family of graphene ribbons, as could be expected: ~ 3.2 eV [173] and ~ 1.5 eV [174], respectively (see Fig. 8).

3.4 Dependence of the electronic structure of graphene ribbons on elastic stresses

One of the methods for modifying the bandgap width of armchair GNRs is to deform the structures in the direction of the vector of translation of the ribbon, which leads to the divergence or convergence of the valence and conduction bands of the GNR (Fig. 9). It has been shown in a number of studies [175–179] that the bandgap width of graphene ribbons can oscillate with a significant amplitude (Fig. 9b). This effect can be explained based on the analysis of the energy-band structure of the ribbons. Indeed, under the action of mechanical stress along the ribbon, its unit cell and the Brillouin zone are deformed (upon compression, the length L_r of the unit cell of the GNR decreases; upon extension, it increases; and the length of the wave vector along the ribbon, $Q_r = \pi/L_r$, increases or decreases accordingly).

Hence, in the Brillouin zone of an undisturbed graphene, the states that are allowed for graphene at the wave vectors nQ_r become shifted relative to the K point, and the branches of the spectrum of a ‘stressed’ GNR move over the graphene cone (see formula (4) for $E(k)$) and vary along with the magnitude of the bandgap (Fig. 9c). When the K point is located in the middle between the states that are allowed for the GNR (point 1 in Fig. 9c), the bandgap width of the ribbon is maximum; when the K point intersects the allowed states, the bandgap vanishes (point 2 in Fig. 9c). The distance between the allowed states is inversely proportional to the ribbon width. The maximum width of the bandgap and the degree of deformation that is

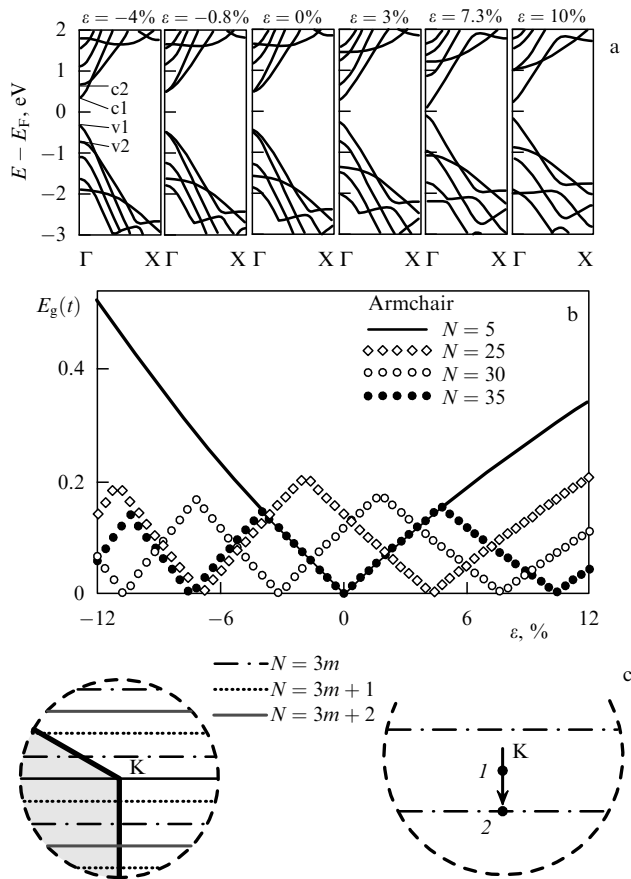


Figure 9. (a) Changes in the energy band structure of a 13-AGNR ribbon under its deformation [176]; (b) widths of the energy gap of GNRs with different indices as functions of the degree of deformation [175]; (c) shift of the allowed states in the Brillouin zone for an armchair graphene ribbon relative to the K point, at which the valence and conduction bands intersect upon deformation of the GNR [180].

necessary to achieve this maximum decrease with increasing the GNR width [180].

Recently, in investigating changes in the electrical resistivity of a free-standing GNR, depending on its deformation, Huang et al. [181] used the method of pushing a GNR by a wedge. Although the experiment did not show a significant increase in the width of its bandgap, apparently because of the large GNR width (1.5 to 4 μm), such experiments with narrower ribbons can probably confirm the theoretical predictions.

3.5 Chemical modification of ribbons

As was shown in Section 3.3, the main difference between graphene ribbons and other sp^2 -type carbon structures (graphene, nanotubes, fullerenes) is the existence of edges, whose shape and type determine the properties of the ribbons. It follows that the electronic and magnetic properties of the ribbons differ sharply depending on which shape—armchair or zigzag—is characteristic of their edges.

It is usually assumed in the investigations that ribbon edges are passivated by hydrogen atoms, and therefore the entire structure preserves the sp^2 hybridization of the carbon atoms. In some studies, however, this fact was doubted: in [182], after considering various ways of passivation of the GNR edges by hydrogen atoms, it was shown that under normal conditions, the energetically most favorable

process is the passivation of a zigzag GNR with alternating monohydrogenated and dihydrogenated sites. The structure with a monohydrogenated passivation is stable only at an extremely low concentration of hydrogen in the environment. In the case of armchair ribbons, under normal conditions, the ribbons that are stable are those with monohydrogenated and dihydrogenated configurations, where each edge atom of carbon is respectively connected with one and two hydrogen atoms. The results obtained are related to Clar's rule, which states that the most stable isomer of a given hydrocarbon molecule is an isomer containing a maximum number of benzene rings—which is characteristic of ribbons with the above-mentioned types of passivation.

The problem of the variation of the electronic properties of ribbons upon the adsorption of various radicals on their edges was considered in a series of studies [184–187]. Most calculations were performed for ribbons with monohydrogenated edges. But the presence of other radicals at the ribbon edges can significantly affect the electronic properties of a structure. This especially refers to zigzag ribbons, because a high concentration of spin density can arise at the edges of precisely these ribbons [167]. Investigations of the stability and electronic properties of graphene ribbons have been performed with various functional groups, e.g., OH, CO_2 , O [184], NH_2 , OH, COOH, NO_2 , O [185], OH, NH_3 , O [186], OH, SH [187].

Critically important for the electronic properties of ribbons upon their functionalization are the ribbon width, the concentration of functional groups at the ribbon edges, and the occurrence of functionalization on one or both edges of the ribbon. For example, a graphene ribbon one of whose edges was monohydrogenated and the other dihydrogenated should reveal ferromagnetic properties according to the predictions in Ref. [188].

We also note that the problem of the stability of the graphene ribbons themselves remains unsolved. It was theoretically shown in [182, 189–192] that the energetically most favorable structure of the zigzag edge of graphene is an atomic structure of the reczag (reconstructed zigzag) type with alternating pentagonal and heptagonal rings (Fig. 10a), with the difference between the energies of the reconstructed edges of the zigzag and reczag types being $0.35 \text{ eV } \text{\AA}^{-1}$ [189]. The authors of Ref. [193] have reported on the experimental confirmation of the existence of such edges (Fig. 10b).

Because the conductivity of GNRs depends on their size, this material is very interesting for its application in nanoelectronics. On the basis of graphene ribbons, field transistors have been designed with the cutoff frequency up to 155 GHz [196]. In addition, it was suggested to use GNRs as memory elements in digital devices [197] and chemical sensors [198].

Already in near future, the relative easiness of fabrication of ribbons of various dimensions will allow using such ribbons as conducting elements in nanodiodes, nanotransistors, and nanocircuits (Fig. 11). In Ref. [199], a trigger circuit based on only graphene ribbons was suggested, in which each element is formed by a combination of ribbons that are cut at different angles or have different widths and/or edges of different types. The analogs of bipolar transistors in such a circuit (VT1, VT2) consist of metallic channels based on zigzag ribbons, which represent a drain and a source, and of short regions of armchair GNRs that are inserted between the drain and the source and serve as a base. In such circuits, the mode of connection between the ribbons is of high

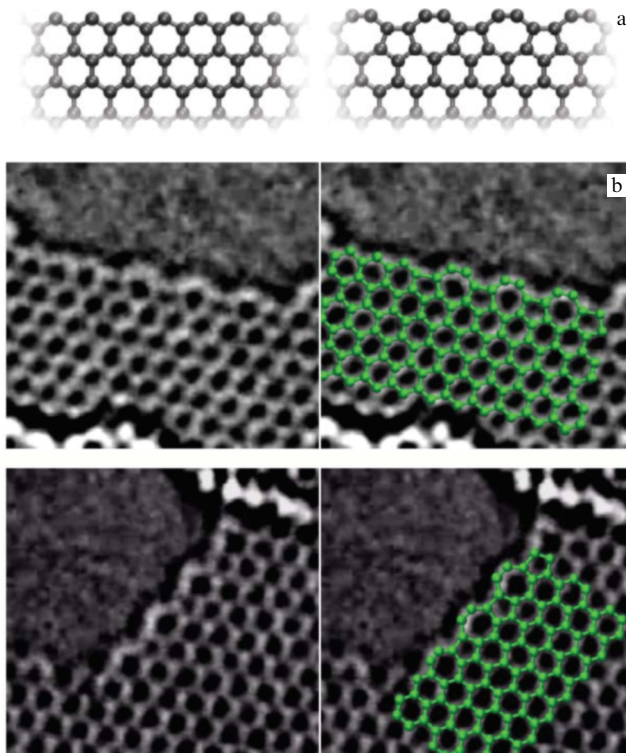


Figure 10. (a) Atomic structure of zigzag and reccag (reconstructed zigzag) edges of graphene [189]; (b) photos of the reccag graphene edges [193].

importance; for example, ribbons connected at an angle of 120° (as in the regions S1 and T1) pass the current almost without reflection, whereas GNRs connected at 60° (regions R1, R2, R3, and R4) play the role of resistors, because they weaken the current by a factor of approximately five per junction.

The current can also be reduced by a sharp change in the ribbon width due to a significant scattering and a decrease in the mobility of charge carriers at the GNR edges [199]. Indeed, the mean free path between two acts of scattering of charge carriers at the edge of a nanoribbon is propor-

tional to W/P , where P is the probability of backward scattering [200].

4. Graphane and fluorographene

An obvious method for the conversion of half-metallic graphene into a semiconductor is the modification of its structure by incorporating defects using methods such as chemisorption of atoms [201, 202], doping [203], producing of vacancies by removing atoms [204–206], or introducing topological Stone–Wales defects [206–208] (in the last cases, a local gap up to 0.3 eV wide appears, which can be very important for creating local semiconducting regions [209]). In this section, we consider the first possibility. Chemisorption of foreign atoms on the surface of graphene leads to a change in the hybridization of carbon atoms from sp^2 to sp^3 , which affects the electronic properties of the material. Indeed, when a carbon atom acquires a fourth neighbor, a σ bond is formed, but then the π system, which is responsible for the conductivity of graphene, is destroyed.

In terms of condensed-matter physics, this effect can be described as a transformation of chemical bonds between atoms of semimetallic graphene into the bonds between atoms of dielectric diamond. When all the bonds between the graphene atoms change their hybridization to sp^3 , the band structure of graphene is transformed into a diamond-like one. In practice, several ways of adsorption of foreign atoms on graphene have been used, in particular, hydrogenation and fluorination. Ideal structures consisting completely of sp^3 carbon atoms are called graphane [210] and fluorographene [211].

4.1 Methods of preparation and stability of structures

The possibility of hydrogenating graphene was first indicated in Ref. [212], where various versions of the distribution of adsorbed hydrogen of the graphene surface were analyzed. It was shown that the energetically most favorable is an armchair structure [210], where all carbon atoms of one sublattice are bound with hydrogen atoms on one surface of the graphene, and the carbon atoms of the other sublattice are bound with the hydrogen atoms on the other side of the

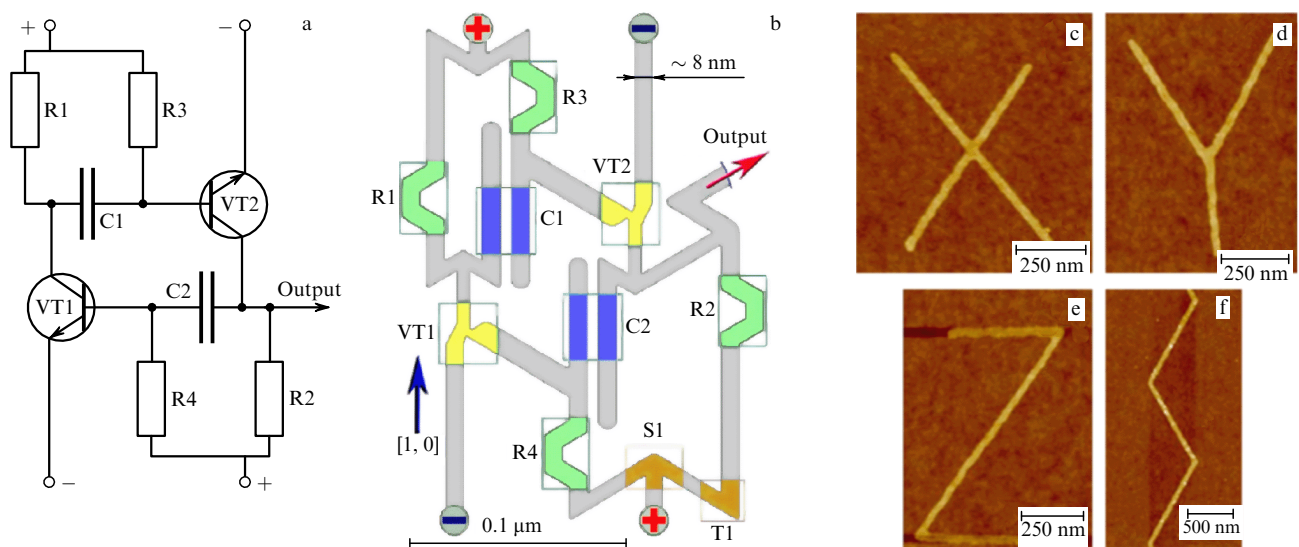
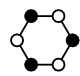
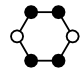
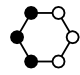


Figure 11. (a) A trigger circuit and (b) its implementation using graphene ribbons [199]; multiterminal graphene ribbons [129]: (c) X, (d) Y, (e) Z, and (f) zigzag types, which can serve as the elements of such a circuit.

Table. Conformers of graphane and fluorographene. The energy ΔE in all the studies was calculated relative to the energy of the most stable armchair configuration. In the images of the conformers, the dark and light dots correspond to hydrogen atoms respectively adsorbed on the upper and lower surfaces of graphane.

Configuration	Space symmetry group (order number of space group)	$\Delta E_{\text{graphane}}$ (eV/atom)	$\Delta E_{\text{fluorographene}}$ (eV/atom)	Structure
Armchair	$P3m1$ (164)	0	0	
Boat	$Pmmm$ (59)	0.10 [212] 0.06 [210], 0.05 [213–215] 0.03 [216]	0.07 [214, 217], 0.08 [215, 216]	
Washboard [214]	$Pmma$ (53)	0.06 [212], 0.05 [213] 0.03 [214–216]	0.04 [214–216]	
Stirrup [216]				

graphene. However, we note that there are a number of conformers of graphane (see the table) with an energy close to that of the armchair structure, which can also be obtained experimentally.

In [218–221], a graphane-like structure was synthesized by adsorption of separate hydrogen atoms on the surface of graphene. The main problem is in the stability of the structure obtained. It was shown in [222] that the process of the formation of graphane islands on graphene becomes energetically favorable only after the island size exceeds ~ 1 nm (or 24 hydrogen atoms assembled into a compact island obeying the aromaticity rule). There are grounds to believe that as a result of synthesis, a structure is formed with graphene roads between graphane regions, rather than a CH structure completely filled with hydrogen, because the samples obtained have an enhanced conductivity [218] compared to the expected dielectric properties of graphane (see Section 4.2). This is confirmed by molecular dynamics simulations of the process of graphane formation from hydrogen atoms [223].

The formation of roads in graphane can be explained by the fact that hydrogen atoms can be adsorbed on one side of graphene in both the A sublattice and the B sublattice. Between the islands of graphane formed in the first and second cases, a graphene region is preserved that is energetically unfavorable for the attachment of hydrogen atoms, because a homogeneous graphane/fluorographene

configurations of the armchair type cannot then be formed (Fig. 12).

The development of a technique for controlling the amount of hydrogen that will be connected to the graphene surface will allow controlling the width of the bandgap of partially hydrogenated graphene (PHG) and hence widely using it in semiconducting nanoelectronics. One of the ways to solve this problem is to synthesize PHG on graphene on a metallic substrate. Indeed, upon the formation of a bond between hydrogen and carbon on the outer side of graphene, the unsaturated sp^3 bonds allow bonds between carbon and metal atoms of the substrate to form. Because the lattice parameters of graphene and the substrate are different, a moiré pattern is formed in such a structure, which determines the subsequent adsorption of hydrogen [224]; this was indeed revealed experimentally in [201] (Fig. 13). Consequently, this method is promising for the production of PHG with semiconducting properties. The problem in the case of such a structure is the presence of a metallic substrate chemically bound to graphane. Apart from the problem of the synthesis of PHG, the problem of separating it from the substrate also arises here.

In the case of fluorographene, the situation concerning the stability is fundamentally different. The binding energy of atoms in a fluorine molecule is significantly less than in a hydrogen molecule, which leads to a higher stability of the fluorographene structure. It was shown in [225] that while the process of hydrogenation at the first stages is energetically unfavorable, the adsorption of fluorine on graphene occurs without a barrier for the nucleation of a new phase.

For the synthesis of fluorographene, the following techniques were used, which, in fact, represent the realization of the two paradigms of nanotechnology: top-down and bottom-up:

(1) the method of splitting a graphite fluoride crystal by the action of ultrasound on graphite fluoride in a solution of isopropyl alcohol [226], sulfolane [227], and dimethylformamide [228], as well as by mechanical splitting using a scotch tape [211, 229] (the top-down paradigm: the macroscopic material is separated to a desired nanostructure—fluorinated graphene sheets);

(2) the method of adsorption of fluorene atoms on graphene [211, 229–231] (the bottom-up paradigm: the necessary nanostructure is synthesized from nanostructures of a smaller size—from graphene layers of angstrom thickness).

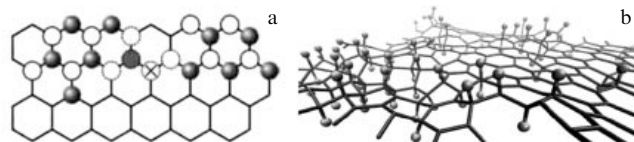


Figure 12. Formation of graphene roads in graphane [223]: (a) layout that helps in explaining the cause of the appearance of graphene roads in the structure in the process of growth of graphane islands on graphene. If the growth begins in different sublattices of graphene, the islands cannot join into a homogeneous armchair configuration, since at the site of their junction a region (denoted by a circle with a cross) arises that is energetically unfavorable for the hydrogen attachment. Gray and white dots denote hydrogen atoms respectively located above and below the graphene sheet. (b) Isometric projection of the graphane structure obtained by a molecular dynamics simulation of its growth. The material is seen to be inhomogeneous; purely graphene regions are observed between hydrogenated islands.

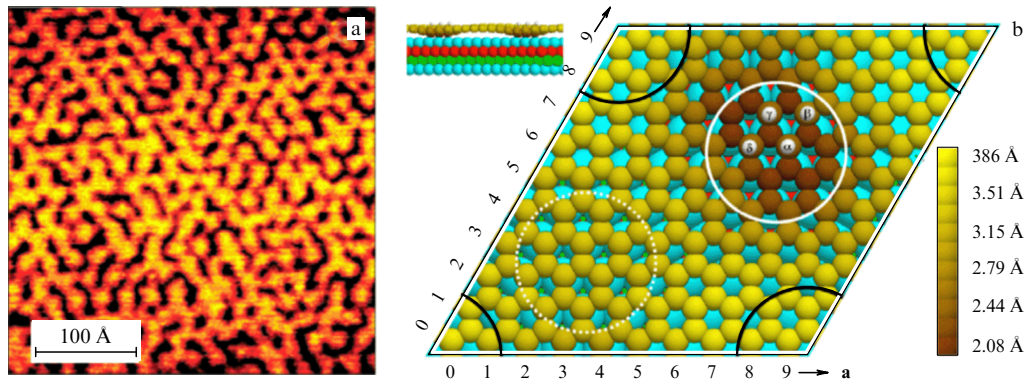


Figure 13. (color online). Partly hydrogenated graphene with hydrogen atoms forming a moiré pattern on the surface of Ir(111): (a) experimental image obtained using scanning tunneling microscopy [201]; (b) theoretical model proposed in Ref. [224]. White circles denote hydrogen atoms; brown circles in a large white circle correspond to carbon atoms connected with both hydrogen and metal atoms; large black circles show carbon atoms forming domes raised over the Ir substrate (blue, red, and green circles respectively denote the first (upper), second, and third surface layers of metal atoms).

4.2 Electronic properties

Because graphane and armchair-type fluorographene can be conventionally represented as a very thin sheet of diamond, these structures should manifest dielectric properties and have a diamond-like energy-band structure (Fig. 14). The widths of the bandgaps of these structures calculated using various theoretical methods were found to range from 3.4 to 6.0 eV for graphane [210, 213, 215, 232–235] and from 3.0 to 7.5 eV for fluorographene; the largest values were obtained by the most precise method of Green's functions. The results of measurements show a significantly narrower width of the bandgap of both the graphane (which follows indirectly from its semiconducting character) [218] and of the fluorographene (for which the values of 2.9 [230], 3.0 [211], and 3.8 eV [231] were obtained). Most probably, this is related to the presence of graphene roads or islands in graphane and fluorographene and to the existence of configurations different from armchair ones.

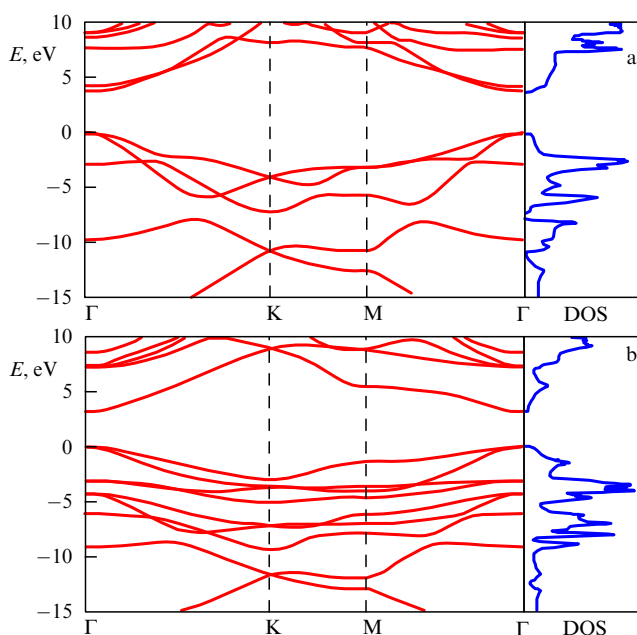


Figure 14. Energy-band structures and the densities of states (DOSs) of (a) graphane and (b) fluorographene [213].

In some studies, the dependence of the electronic properties of hydrogenated graphene on the concentration and location of adsorbed hydrogen atoms has been studied. Having considered the possible variants of the location of hydrogen on graphene, the authors of those studies arrived at the following conclusions:

(1) the bandgap width of PHG decreases monotonically according to a polynomial law (a third-degree polynomial) with decreasing the hydrogen concentration and reaches zero at 66.67% [236];

(2) the bandgap width of PHG decreases nonmonotonically, and PHG passes into a metallic state with decreasing the hydrogen concentration to 80% [237].

We see that there is currently no complete agreement concerning this question. It can be supposed that the main contribution to the observed dependences of the bandgap width of PHGs on the concentration of hydrogen at large concentrations of chemisorbed hydrogen comes from unfilled graphene roads, whose electronic properties depend nonmonotonically on the structure parameters. In the case of small hydrogen concentrations, the available hydrogen islands can be regarded as defects—disturbances of the graphene structure. More detailed information on these objects is given in Section 5.2.

Nevertheless, in spite of the incomplete clarity on the question of the electronic properties of fluorographene, a transistor based on it has already been developed, and it was shown that fluorination significantly increases the resistivity of the material [229].

After the hydrogenation of graphene, there quite naturally arose the problem of the existence of graphane ribbons. In theoretical work [238–240], zigzag and armchair graphane ribbons with edges passivated by hydrogen atoms were considered. Just as graphane itself, ribbons of both types are wide-bandgap semiconductors. The bandgap of ribbons is greater than that of graphane because of the quantum size effect; however, this effect weakens with increasing the ribbon width; the energy gap decreases, tending to the one for graphane [238–240]. Currently, there are no experimental data on the synthesis of graphane ribbons, although Talyzin et al. [141] stated that when fabricating graphene ribbons by cutting carbon nanotubes using hydrogen, the latter can attach not only to the edges of the arising GNRs but also to their surface, which can lead to the appearance of graphane ribbons.

4.3 Diamanes

Graphane (and fluorographene) can be regarded as only one of the first representatives of a series of diamond-like films CH_x with a (111) surface covered by hydrogen (or fluorine). Currently, extended experimentally obtained diamond films usually have a thickness of a few microns [241], at which quantum effects do not affect the electronic structure of the material. But in the case of nanometer thicknesses, the quantum effect should play a decisive role. The hypothetical structures of such $\text{CH}(\text{C}_2\text{H})$ films that are formed of two (three) graphene layers with the complete bonding of the C atoms between themselves and with their surfaces being

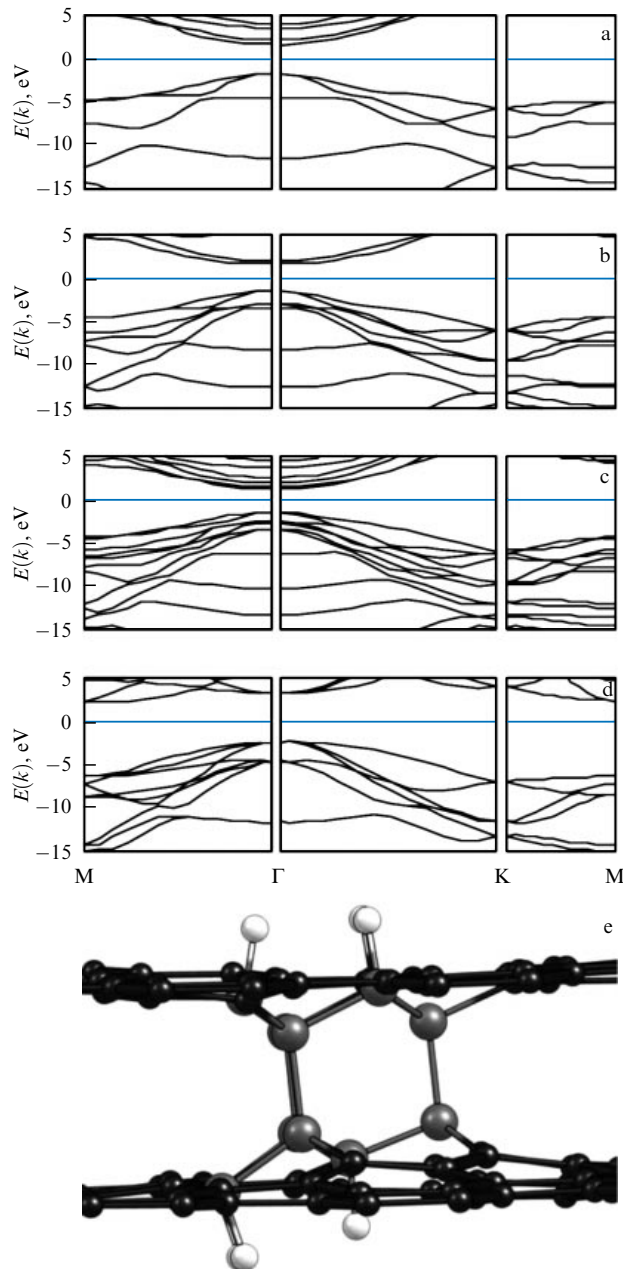


Figure 15. Evolution of the energy band structure of two-dimensional carbon materials: (a) graphane; (b) bilayer diamane; (c) trilayer diamane; (d) diamond [232] ($E = 0$ corresponds to the Fermi level); (e) schematic view of the formation of a diamane nucleus on bigraphene: hydrogen atoms (white balls) are deposited on its two sides provoking ‘gluing’ of C atoms located in neighboring layers (gray balls) lying on top of one another [242].

covered by chemisorbed H atoms are called diamanes [242]. Graphane and the diamanes represent a continuous series of diamond-like structures with a gradually increasing thickness. Their energy-band structures are similar and have features in common with the electronic spectrum of diamond (Figs 15a–15d).

An interesting feature is the direct-gap character of the energy bands of these nanostructures; due to this feature, they can be used as active media for lasers [232]. Calculations [243] show that by applying an electric field up to $\sim 1.3 \text{ V \AA}^{-1}$ perpendicular to the plane of a diamane, its bandgap can be decreased to zero. However, this result is doubtful because the authors of [243] have not considered the stability of the atomic structure itself in such a strong field (up to 10^5 kV cm^{-1}).

It is supposed that diamanes can form when bigraphene is placed in the hydrogen discharge plasma; then, under the corresponding conditions (pressure and temperature of hydrogen), the hydrogen atoms become chemisorbed on both surfaces of bigraphene [242, 244]. Thus, a carbon atom of the ‘upper’ graphene that is not located over a C atom of the ‘lower’ graphene and, consequently, is more ‘free’, after the attachment of a hydrogen atom leaves the plane because of the sp^3 hybridization. The three surrounding C atoms move down somewhat (Fig. 15e). Such a rearrangement also occurs with the atoms of the ‘lower’ graphene, and therefore the C atoms of neighboring layers located over one another also undergo sp^3 hybridization. This leads to the formation of a nucleus of diamane (Fig. 15e).

We note experimental studies [245–248] whose authors reported the observation of C_2F films; in [246], these films were interpreted as ‘diamane’ films with the surface passivated by fluorine atoms.

Because of the small thickness and good mechanical properties, the dielectric diamane films should find wide application in both electronics and optics.

5. Graphene-based electronic superlattices and waveguides

In Refs [249–252], the possibility was shown for the first time of creating ‘nanoroads’ on a graphene sheet — graphene nanostripes bounded from both sides by a kind of diamond-like line with a high potential barrier arising upon the transformation of sp^2 -hybridized C atoms of graphene into sp^3 C atoms due to the adsorption of pairs of H atoms; their electronic properties have been calculated. In Ref. [253], a structure of the graphene nanoroads has been suggested, and in the work of Yakobson’s research group, the electronic properties of such nanoroads bounded from both sides by nanostripes of graphane [254] or fluorographene [225] have been calculated.

These objects can be represented as electron waveguides — analogs of graphene ribbons with very close electronic properties. We also note the existence of a large barrier for diffusion of ‘bounded’ H atoms near the graphene–graphene interface (estimated as 1 eV in [255] and 2–3 eV in [222, 256, 257]). Therefore, it can be expected that such structures will have sufficient thermal stability to be applicable in practice.

It was noted in Ref. [258], that the presence of physically adsorbed polar molecules H_2O , HF, and NH_3 on a graphene surface facilitates the migration of chemically attached hydrogen atoms, lowering the barrier for migration by a factor of approximately two. According to [258], this effect

can permit more efficiently forming a homogeneous graphane structure from randomly adsorbed hydrogen islands on graphene.

In the literature, variants of the formation of superlattices on graphene due to the effect of interaction with the substrate or due to an external potential are also considered. Ratnikov [259] has considered a superlattice on graphene located on a substrate of alternating nanolayers of silicon dioxide and hexagonal boron nitride. However, this variant is difficult to implement; on the other hand, the opening of a gap of graphene due to the action of a BN layer is very weak (~ 0.005 eV) [260, 261], which gives a very small effect. In addition, there were a number of other hypothetical superlattices with a one-dimensional periodic potential (induced by an electric field [262–264] or by corrugations on graphene [265–267]), which in fact face the same difficulties in practical realization.

5.1 Chains of hydrogen atoms on graphene

The graphane regions with sp^3 -hybridized C atoms create a significant energy barrier for the penetration of free electrons in neighboring graphene regions. It is important to note that the barrier is virtually independent of the width of the graphane region, which can therefore be decreased to a single chain of adsorbed hydrogen atoms. This structure with adsorbed hydrogen atoms on one side of graphene (Fig. 16a), which was suggested in [249], is supported by the experimental facts of chemisorption of pairs [268] and linear chains of hydrogen atoms [269] on the graphite surface.

Graphene roads bounded by chains of adsorbed hydrogen atoms demonstrate electronic properties close to those of graphene ribbons. For example, the bandgap width of such structures oscillates with changing the distance between the chains [250] (Fig. 16b), which was confirmed experimentally by the observation of a decrease in the surface conductivity in the region between adsorbed chains of hydrogen atoms [269]. Of great interest is the possibility of using them to create superlattices in which a ‘quasi-metallic’ stripe with a smaller bandgap is separated from both sides by stripes with larger bandgaps (Fig. 16c). Thus, it is possible to create an electron waveguide on graphene—a kind of a quantum nanometer wire with ‘one atom’ thickness (Fig. 16d).

If the chain becomes broken, the width of the bandgap of the structure decreases to zero nonmonotonically. Therefore, it can be expected that in the case of periodic adsorption of hydrogen molecules on graphene, it is possible to vary the semiconducting properties of the material [251]. The bandgap of the structure, just as in the case of graphene ribbons, can change within wide limits, up to 80%, under the action of a tensile or compressive mechanical stress directed across the chains [252] (Fig. 16b).

5.2 Graphene roads on graphane and fluorographene

As was said above, there are solid grounds to believe that incomplete hydrogenation (fluorination) of graphene occurs upon synthesis; and roads of graphene can be created between the graphane or fluorographene regions. We note the experiment reported in [270], in which graphene was subjected to the action of an electron beam (which led to a significant decrease in the graphene resistivity), as well as the experiment in [271], where a graphene nanoroad on graphene oxide was obtained by ‘rubbing off’ oxygen using the heated tip of an electron-probe microscope. The properties of graphene roads in graphane and fluorographene were

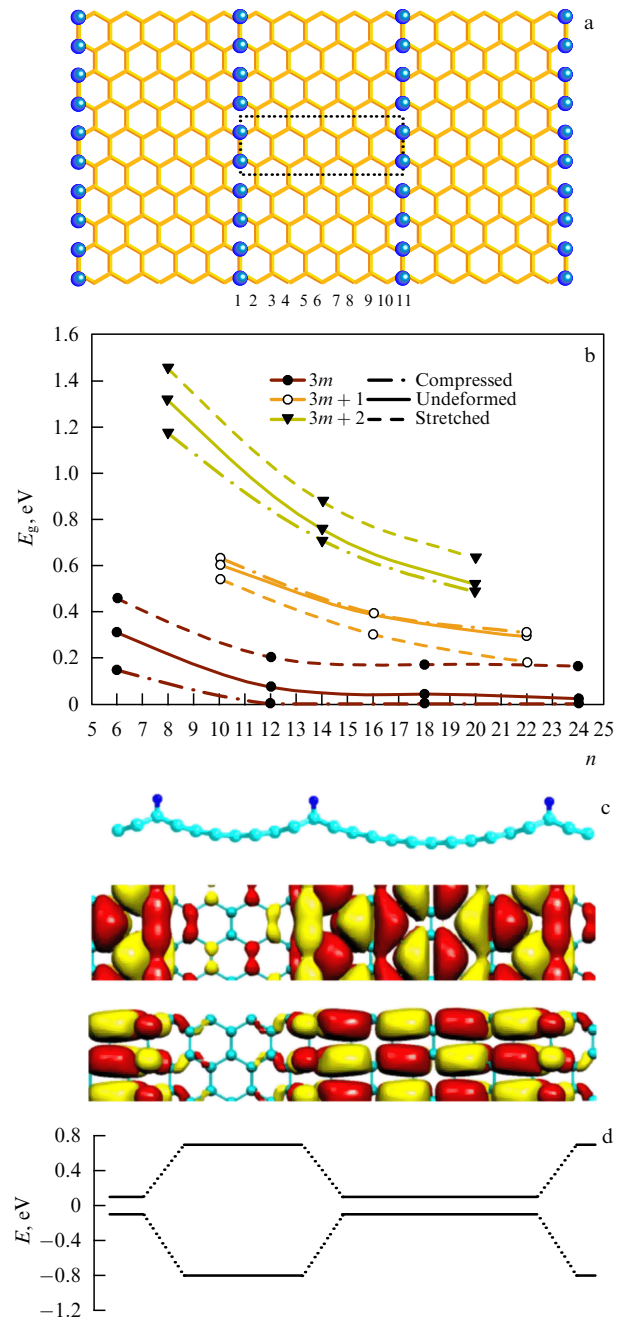


Figure 16. (a) Atomic structure of graphene roads bounded by chains of adsorbed hydrogen atoms. (b) Dependence of the energy gap of the structure on the distance between the chains and on the mechanical stress (degree of deformation, 2%) applied in the direction perpendicular to the chains [252]. (c) Atomic structure of graphene roads formed by chains of hydrogen atoms located at different distances from one another. (d) Distribution of the wave function near the top of the valence band and near the bottom of the conduction band in the structures and a schematic of a heterojunction in the superlattice: dependences of the energy gap width on the period of the superlattice [250].

respectively studied theoretically in Refs [254] and [255]. These objects can be represented as graphene ribbons bounded on both sides by high potential barriers formed by graphane (fluorographene). It can therefore be expected that the electronic properties of graphene roads are similar to those of graphene ribbons (see Section 3.3). Calculations show that the properties of armchair and zigzag roads are similar to those of the corresponding ribbons. In the case of

an armchair road, its bandgap oscillates upon changing its width (the number n). But in contrast to GNRs, in which $E_g^{3m+1} > E_g^{3m} > E_g^{3m+2}$ [see Eqn (7)], the bandgap of the roads obeys the inequalities $E_g^{3m} > E_g^{3m+1} > E_g^{3m+2}$ in view of the specific features of the distortion of their boundaries. The magnitudes of the bandgaps of the corresponding graphene ribbons in graphane and fluorographane are approximately equal to one another.

In the case of a zigzag road, just as in the case of a GNR, the structure with an antiferromagnetic ordering of spins is more favorable. It manifests semiconducting properties with a bandgap monotonically decreasing with increasing the width of the road [225, 254].

In the work of Tour's research group [202], a successful synthesis of graphene–graphane structures was reported, but the micron width of the roads obtained prevented obtaining properties predicted in the theory.

5.3 Graphene-ribbon-based superlattices

The fact that there is a dependence of the bandgap of GNRs (as well as of the bandgaps of graphene roads in graphane/fluorographane structures) on the size of the structures suggests the possibility of constructing heterostructures and heterojunctions on their basis.

For example, the authors of [272] studied properties of superlattices obtained by combining zigzag stripes of various widths and demonstrated changes in spin polarizations of the stripes upon their combination. It turned out that in the wide part of the superlattice, the spin polarization disappears and the narrow part has antiferromagnetic properties (Fig. 17a). In another study by the same research group [273], super-

lattices consisting of armchair stripes were examined. It was revealed that in segments containing wider stripes, a localization of electron density occurs and, thus, quantum dots are formed (Fig. 17b).

The above-described method of production of graphene ribbons by cutting carbon nanotubes also allows obtaining superlattices with a hybrid structure (... – CNT – GNR – CNT – ...) in which nanotubes having a half-metallic conductivity alternate with semiconducting graphene ribbons. The electronic and transport properties of such structures have been investigated in a number of studies [134, 274, 275], in which the following interesting properties have been found: in [274], it was noted that the application of a transverse electric field changes the conduction type from semiconducting to semi-metallic. In [134], it was shown that such objects can have a significant magnetoresistance. If the edges of a graphene ribbon in a hybrid structure of the ... – CNT – GNR – CNT – ... type is monohydrogenated on one side and dihydrogenated on the other side, then, as was shown in [275], such a ribbon can be used as a spin filter.

6. Conclusions

In this review, we discussed the state of the art in the field of investigations of the physics of graphene-based materials that have a semiconducting conductivity type. We considered semiconducting graphene-based nanostructures, which, in our opinion, are the most promising for further study and application. These are objects such as graphene ribbons of nanometer width, as well as materials obtained by the modification of graphene using complete or partial hydrogenation/fluorination of its surface (graphane, fluorographane, and diamane). The methods of production of such structures and their electronic and conducting properties were considered in detail, and the prospects for their further application were discussed.

Investigations of graphene are undoubtedly only at the initial stage of development; however, we hope that progress in this field will lead to a situation where integrated circuits based on graphene and its derivatives will play the main role in electronic devices in the nearest future.

Acknowledgments

This work was supported in part by the Russian Foundation for Basic Research (RFBR project No. 11-02-01453a) and by the Russian–German Foundation (grant No. DFG436RUS 113/990/0-1). One of us (PBS) also thanks the RFBR (project No. 12-02-31261) and the Ministry of Education and Science of the Russian Federation (Contract No. 14.B37.21.1645) for support.

References

1. Kroto H W et al. *Nature* **318** 162 (1985)
2. Osawa E *Kagaku Kyoto* **25** 854 (1970)
3. Bochvar D A, Gal'pern E G *Proc. Acad. Sci. USSR* **209** 239 (1973) [*Dokl. Akad. Nauk SSSR* **209** 610 (1973)]
4. Iijima S *Nature* **354** 56 (1991)
5. Kosakovskaya Z Ya, Chernozatonskii L A, Fedorov E A *JETP Lett.* **56** 26 (1992) [*Pis'ma Zh. Eksp. Teor. Fiz.* **56** 26 (1992)]
6. Khvostov V V et al. *JETP Lett.* **56** 277 (1992) [*Pis'ma Zh. Eksp. Teor. Fiz.* **56** 280 (1992)]
7. Chernozatonskii L A et al. *JETP Lett.* **57** 35 (1993) [*Pis'ma Zh. Eksp. Teor. Fiz.* **57** 35 (1993)]
8. Ebbesen T W, Ajayan P M *Nature* **358** 220 (1992)
9. Chernozatonskii L A et al. *Chem. Phys. Lett.* **228** 94 (1994)

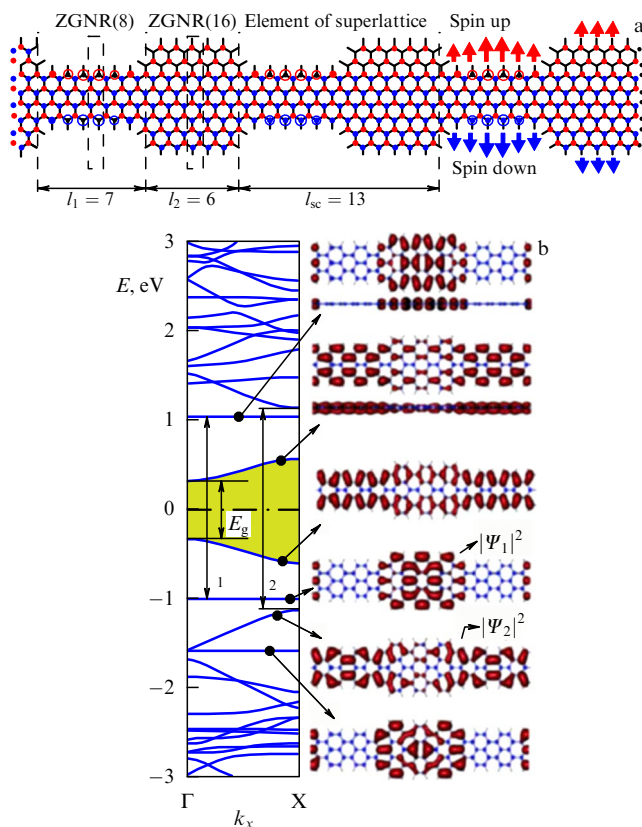


Figure 17. (a) Spin polarization for zigzag superlattices [272]; (b) energy band structure and charge distribution in selected regions [273].

10. Iijima S, Ichihashi T *Nature* **363** 603 (1993)
11. Bethune D S et al. *Nature* **363** 605 (1993)
12. Radushkevich L V, Luk'yanovich V M *Zh. Fiz. Khim.* **26** 88 (1952)
13. Davis W R, Slawson R J, Rigby G R *Nature* **171** 756 (1953)
14. Oberlin A, Endo M, Koyama T *Carbon* **14** 133 (1976)
15. Oberlin A, Endo M, Koyama T *J. Cryst. Growth* **32** 335 (1976)
16. Nesterenko A M et al. *Izv. Akad. Nauk SSSR Met.* (3) 12 (1982)
17. Abrahamson J, Wiles P G, Rhoades B L *Carbon* **37** 1873 (1999)
18. Jones D E H *New Scientist* **32** 245 (1966)
19. Kornilov M Yu *Khim. Zhizn'* (8) 22 (1985)
20. Shelton J C, Patil H R, Blakely J M *Surf. Sci.* **43** 493 (1974)
21. Isett L C, Blakely J M *Surf. Sci.* **58** 397 (1976)
22. Eizenberg M, Blakely J M *Surf. Sci.* **82** 228 (1979)
23. Eizenberg M, Blakely J M *J. Chem. Phys.* **71** 3467 (1979)
24. Oshima C et al. *Jpn. J. Appl. Phys.* **16** 965 (1977)
25. Zi-Pu H et al. *Surf. Sci.* **180** 433 (1987)
26. Kholin N A, Rut'kov E V, Tontegode A Y *Surf. Sci.* **139** 155 (1984)
27. Gall' N R et al. *Sov. Phys. Solid State* **27** 1410 (1985) [*Fiz. Tverd. Tela* **27** 2351 (1985)]
28. Rut'kov E V, Tontegode A Ya *Surf. Sci.* **161** 373 (1985)
29. Oshima C, Nagashima A *J. Phys. Condens. Matter* **9** 1 (1997)
30. Nagashima A et al. *Surf. Sci.* **291** 93 (1993)
31. Berger C et al. *J. Phys. Chem. B* **108** 19912 (2004)
32. Boehm V H P et al. *Z. Naturforsch. B* **17** 150 (1961)
33. Novoselov K S et al. *Science* **306** 666 (2004)
34. Novoselov K S et al. *Proc. Natl. Acad. Sci. USA* **102** 10451 (2005)
35. Novoselov K S et al. *Nature* **438** 197 (2005)
36. *Nature Mater.* **6** 169 (2007)
37. Wallace P R *Phys. Rev.* **71** 622 (1947)
38. McClure J W *Phys. Rev.* **104** 666 (1956)
39. Slonczewski J C, Weiss P R *Phys. Rev.* **109** 272 (1958)
40. Boehm H-P, Setton R, Stumpp E *Pure Appl. Chem.* **66** 1893 (1994)
41. Meyer J C et al. *Nature* **446** 60 (2007)
42. Katsnelson M I *Mater. Today* **10** (1–2) 20 (2007)
43. Morozov S V, Novoselov K S, Geim A K *Phys. Usp.* **51** 744 (2008) [*Usp. Fiz. Nauk* **178** 776 (2008)]
44. Castro Neto A H et al. *Rev. Mod. Phys.* **81** 109 (2009)
45. Allen M J, Tung V C, Kaner R B *Chem. Rev.* **110** 132 (2010)
46. Avouris P *Nano Lett.* **10** 4285 (2010)
47. Dresselhaus M S, Araujo P T *ACS Nano* **4** 6297 (2010)
48. Biró L P, Lambin P *Carbon* **48** 2677 (2010)
49. Novoselov K S *Rev. Mod. Phys.* **83** 837 (2011); *Usp. Fiz. Nauk* **181** 1299 (2011)
50. Sun Z, James D K, Tour J M *J. Phys. Chem. Lett.* **2** 2425 (2011)
51. Zhu Y et al. *Adv. Mater.* **22** 3906 (2010)
52. Choi W et al. *Critical Rev. Solid State Mater. Sci.* **35** 52 (2010)
53. Eletskii A V et al. *Phys. Usp.* **54** 227 (2011) [*Usp. Fiz. Nauk* **181** 233 (2011)]
54. Wei D, Liu Y *Adv. Mater.* **22** 3225 (2010)
55. Grayfer E D et al. *Russ. Chem. Rev.* **80** 751 (2011) [*Usp. Khim.* **80** 784 (2011)]
56. Making Graphene 101, Ozyilmaz' Group, <http://youtu.be/rphiCdR68TE>
57. Fujibayashi Y *J. Phys. Soc. Jpn.* **34** 989 (1973)
58. Fujibayashi Y, Mizushima S *Carbon* **10** 355 (1972)
59. Ohashi Y et al. *Carbon* **36** 475 (1998)
60. Bunch J S et al. *Nano Lett.* **5** 287 (2005)
61. Zhang Y et al. *Phys. Rev. Lett.* **94** 176803 (2005)
62. Geim A K, Novoselov K S *Nature Mater.* **6** 183 (2007)
63. Blake P et al. *Appl. Phys. Lett.* **91** 063124 (2007)
64. Ferrari A C et al. *Phys. Rev. Lett.* **97** 187401 (2006)
65. Rao R et al. *ACS Nano* **5** 1594 (2011)
66. Graf D et al. *Nano Lett.* **7** 238 (2007)
67. Graf D et al. *Solid State Commun.* **143** 44 (2007)
68. Ni Z et al. *Nano Res.* **1** 273 (2008)
69. Casiraghi C et al. *Nano Lett.* **9** 1433 (2009)
70. Krauss B et al. *Nano Lett.* **10** 4544 (2010)
71. Dresselhaus M S, Dresselhaus G *Adv. Phys.* **51** 1 (2002)
72. Shioyama H *J. Mater. Sci. Lett.* **20** 499 (2001)
73. Viculis L M, Mack J J, Kaner R B *Science* **299** 1361 (2003)
74. Horiuchi S et al. *Appl. Phys. Lett.* **84** 2403 (2004)
75. Aizawa T et al. *Phys. Rev. Lett.* **64** 768 (1990)
76. Rosei R et al. *Phys. Rev. B* **28** 1161 (1983)
77. Papagno L, Caputi L S *Phys. Rev. B* **29** 1483 (1984)
78. Miniussi E et al. *Phys. Rev. Lett.* **106** 216101 (2011)
79. Oznuluer T et al. *Appl. Phys. Lett.* **98** 183101 (2011)
80. Lee Y et al. *Nano Lett.* **10** 490 (2010)
81. Gao L, Guest J R, Guisinger N P *Nano Lett.* **10** 3512 (2010)
82. Wofford J M et al. *Nano Lett.* **10** 4890 (2010)
83. Yao Y et al. *J. Phys. Chem. C* **115** 5232 (2011)
84. Ruan G et al. *ACS Nano* **5** 7601 (2011)
85. Bae S et al. *Nature Nanotechnol.* **5** 574 (2010)
86. Himpfel F J et al. *Surf. Sci. Lett.* **115** L159 (1982)
87. Sutter P et al. *Nano Lett.* **9** 2654 (2009)
88. Liao Q et al. *Nanotechnology* **22** 125303 (2011)
89. Hamilton J C, Blakely J M *Surf. Sci.* **91** 199 (1980)
90. Eom D et al. *Nano Lett.* **9** 2844 (2009)
91. Sicot M et al. *Appl. Phys. Lett.* **96** 093115 (2010)
92. Wang B et al. *Nano Lett.* **11** 424 (2011)
93. Rodríguez-Manzo J A, Pham-Huu C, Banhart F *ACS Nano* **5** 1529 (2011)
94. Nag A et al. *ACS Nano* **4** 1539 (2010)
95. Warner J H et al. *ACS Nano* **4** 1299 (2010)
96. Shi Y et al. *Nano Lett.* **10** 4134 (2010)
97. Song L et al. *Nano Lett.* **10** 3209 (2010)
98. Teweldebrhan D, Goyal V, Balandin A A *Nano Lett.* **10** 1209 (2010)
99. Splendiani A et al. *Nano Lett.* **10** 1271 (2010)
100. Lee C et al. *ACS Nano* **4** 2695 (2010)
101. Tusche C, Meyerheim H L, Kirschner J *Phys. Rev. Lett.* **99** 026102 (2007)
102. Ye J et al. *Appl. Phys. Lett.* **98** 263101 (2011)
103. Pouloupoulos P et al. *J. Phys. Chem. C* **115** 14839 (2011)
104. Lin S S *J. Phys. Chem. C* **116** 3951 (2012)
105. Nakano H et al. *Angew. Chem. Int. Ed.* **45** 6303 (2006)
106. Huang P Y et al. *Nano Lett.* **12** 1081 (2012)
107. Tang H, Ismail-Beigi S *Phys. Rev. Lett.* **99** 115501 (2007)
108. Lebègue S, Eriksson O *Phys. Rev. B* **79** 115409 (2009)
109. Houssa M et al. *Appl. Phys. Lett.* **96** 082111 (2010)
110. Cahangirov S et al. *Phys. Rev. Lett.* **102** 236804 (2009)
111. Wang S *J. Phys. Soc. Jpn.* **79** 064602 (2010)
112. Li H et al. *J. Phys. Chem. C* **114** 11390 (2010)
113. Artyukhov V I, Chernozatonskii L A *J. Phys. Chem. C* **114** 9678 (2010)
114. Wakabayashi K et al. *Phys. Rev. B* **59** 8271 (1999)
115. Fujita M et al. *J. Phys. Soc. Jpn.* **65** 1920 (1996)
116. Nakada K et al. *Phys. Rev. B* **54** 17954 (1996)
117. Chen Z et al. *Physica E* **40** 228 (2007)
118. Han M Y et al. *Phys. Rev. Lett.* **98** 206805 (2007)
119. Tapasztó L et al. *Nature Nanotechnol.* **3** 397 (2008)
120. Liang X et al. *Nano Lett.* **10** 2454 (2010)
121. Bai J et al. *Nature Nanotechnol.* **5** 190 (2010)
122. Bai J, Duan X, Huang Y *Nano Lett.* **9** 2083 (2009)
123. Sidorov A N et al. *Nanotechnology* **18** 135301 (2007)
124. Li X et al. *Science* **319** 1229 (2008)
125. Ci L et al. *Nano Res.* **1** 116 (2008)
126. Campos L C et al. *Nano Lett.* **9** 2600 (2009)
127. Datta S S et al. *Nano Lett.* **8** 1912 (2008)
128. Tian J et al. *Nano Lett.* **11** 3663 (2011)
129. Wang X, Dai H *Nature Chem.* **2** 661 (2010)
130. Nemes-Incze P et al. *Nano Res.* **3** 110 (2010)
131. Yang R et al. *Adv. Mater.* **22** 4014 (2010)
132. Weng L et al. *Appl. Phys. Lett.* **93** 093107 (2008)
133. Elías A L et al. *Nano Lett.* **10** 366 (2010)
134. Santos H, Chico L, Brey L *Phys. Rev. Lett.* **103** 086801 (2009)
135. Gutiérrez H R et al. *Nano Lett.* **5** 2195 (2005)
136. Zhang M et al. *Nanostruct. Mater.* **10** 1145 (1998)
137. Cano-Márquez A G et al. *Nano Lett.* **9** 1527 (2009)
138. Kosynkin D V et al. *Nature* **458** 872 (2009)
139. Higginbotham A L et al. *ACS Nano* **4** 2059 (2010)
140. Kosynkin D V et al. *ACS Nano* **5** 968 (2011)
141. Talyzin A V et al. *ACS Nano* **5** 5132 (2011)
142. Jiao L et al. *Nature Nanotechnol.* **5** 321 (2010)
143. Wang X et al. *Nature Nanotechnol.* **6** 563 (2011)
144. Jiao L et al. *Nature* **458** 877 (2009)
145. Jiao L et al. *Nano Res.* **3** 387 (2010)
146. Cai J et al. *Nature* **466** 470 (2010)

147. Chuvilin A et al. *Nature Mater.* **10** 687 (2011)
148. Talyzin A V et al. *Nano Lett.* **11** 4352 (2011)
149. Biró L P, Hevesi L, Lambin P *Nanopages* **5** 1 (2010)
150. Kovacic P, Kyriakis A J. *Am. Chem. Soc.* **85** 454 (1963)
151. Bailey W J, Liao C-W J. *Am. Chem. Soc.* **77** 992 (1955)
152. Murakami M, Iijima S, Yoshimura S J. *Appl. Phys.* **60** 3856 (1986)
153. Wakabayashi K, in *Carbon-based Magnetism. An Overview of the Magnetism of Metal Free Carbon-based Compounds and Materials* (Eds T Makarova, F Palacio) (Amsterdam: Elsevier, 2006) p. 279
154. Dresselhaus M S, Dresselhaus G, Saito R *Carbon* **33** 883 (1995)
155. Kobayashi K *Phys. Rev. B* **48** 1757 (1993)
156. Suenaga K, Koshino M *Nature* **468** 1088 (2010)
157. Hamada N, Sawada S, Oshiyama A *Phys. Rev. Lett.* **68** 1579 (1992)
158. Saito R et al. *Phys. Rev. B* **46** 1804 (1992)
159. Ouyang M et al. *Science* **292** 702 (2001)
160. Son Y-W, Cohen M L, Louie S G *Phys. Rev. Lett.* **97** 216803 (2006)
161. Barone V, Hod O, Scuseria G E *Nano Lett.* **6** 2748 (2006)
162. Yang L et al. *Phys. Rev. Lett.* **99** 186801 (2007)
163. Wang Z F et al. *Phys. Rev. B* **75** 113406 (2007)
164. Lee H et al. *Phys. Rev. B* **72** 174431 (2005)
165. Pisani L et al. *Phys. Rev. B* **75** 064418 (2007)
166. Blase X et al. *Phys. Rev. B* **51** 6868 (1995)
167. Son Y-W, Cohen M L, Louie S G *Nature* **444** 347 (2006)
168. Kan E-J et al. *Appl. Phys. Lett.* **91** 243116 (2007)
169. Shemella P et al. *Appl. Phys. Lett.* **91** 042101 (2007)
170. Rudberg E, Salek P, Luo Y *Nano Lett.* **7** 2211 (2007)
171. Ritter K A, Lyding J W *Nature Mater.* **8** 235 (2009)
172. Tao C et al. *Nature Phys.* **7** 616 (2011)
173. Simonsen A C, Rubahn H-G *Nano Lett.* **2** 1379 (2002)
174. Mondal R, Shah B K, Neckers D C *J. Am. Chem. Soc.* **128** 9612 (2006)
175. Chang C P et al. *J. Appl. Phys.* **101** 063506 (2007)
176. Sun L et al. *J. Chem. Phys.* **129** 074704 (2008)
177. Lu Y, Guo J *Nano Res.* **3** 189 (2010)
178. Liao W H et al. *Eur. Phys. J. B* **76** 463 (2010)
179. Peng X, Velasquez S *Appl. Phys. Lett.* **98** 023112 (2011)
180. Li Y et al. *Nano Res.* **3** 545 (2010)
181. Huang M et al. *Nano Lett.* **11** 1241 (2011)
182. Wassmann T et al. *Phys. Rev. Lett.* **101** 096402 (2008)
183. Clar E *Polycyclic Hydrocarbons* (London: Academic Press, 1964) [Translated into Russian (Moscow: Khimiya, 1971)]
184. Hod O et al. *Nano Lett.* **7** 2295 (2007)
185. Cervantes-Sodi F et al. *Phys. Rev. B* **77** 165427 (2008)
186. Seitsonen A P et al. *Phys. Rev. B* **82** 115425 (2010)
187. Wagner P et al. *Phys. Rev. B* **84** 134110 (2011)
188. Kusakabe K, Maruyama M *Phys. Rev. B* **67** 092406 (2003)
189. Koskinen P, Malola S, Häkkinen H *Phys. Rev. Lett.* **101** 115502 (2008)
190. Huang B et al. *Phys. Rev. Lett.* **102** 166404 (2009)
191. Reddy C D et al. *Appl. Phys. Lett.* **94** 101904 (2009)
192. Rodrigues J N B et al. *Phys. Rev. B* **84** 155435 (2011)
193. Koskinen P, Malola S, Häkkinen H *Phys. Rev. B* **80** 073401 (2009)
194. Yan Q et al. *Nano Lett.* **7** 1469 (2007)
195. Lemme M C et al. *IEEE Electron Device Lett.* **28** 282 (2007)
196. Wu Y et al. *Nature* **472** 74 (2011)
197. Gunlycke D et al. *Nano Lett.* **7** 3608 (2007)
198. Sun S-J *Phys. Rev. B* **75** 165408 (2007)
199. Areshkin D A, White C T *Nano Lett.* **7** 3253 (2007)
200. Wang X et al. *Phys. Rev. Lett.* **100** 206803 (2008)
201. Balog R et al. *Nature Mater.* **9** 315 (2010)
202. Sun Z et al. *Nature Commun.* **2** 559 (2011)
203. Ci L et al. *Nature Mater.* **9** 430 (2010)
204. Chernozatonskii L A et al. *JETP Lett.* **84** 115 (2006) [*Pis'ma Zh. Eksp. Teor. Fiz.* **84** 141 (2006)]
205. Pedersen T G et al. *Phys. Rev. Lett.* **100** 136804 (2008)
206. Appelhans D J, Carr L D, Lusk M T *New J. Phys.* **12** 125006 (2010)
207. Peng X, Ahuja R *Nano Lett.* **8** 4464 (2008)
208. Lahiri J et al. *Nature Nanotechnol.* **5** 326 (2010)
209. Banhart F, Kotakoski J, Krashenninnikov A V *ACS Nano* **5** 26 (2011)
210. Sofo J O, Chaudhari A S, Barber G D *Phys. Rev. B* **75** 153401 (2007)
211. Nair R R et al. *Small* **6** 2877 (2010)
212. Sluiter M H F, Kawazoe Y *Phys. Rev. B* **68** 085410 (2003)
213. Leenaerts O et al. *Phys. Rev. B* **82** 195436 (2010)
214. Artyukhov V I, Chernozatonskii L A *J. Phys. Chem. A* **114** 5389 (2010)
215. Samarakoon D K et al. *Small* **7** 965 (2011)
216. Bhattacharya A et al. *Phys. Rev. B* **83** 033404 (2011)
217. Charlier J-C, Gonze X, Michenaud J-P *Phys. Rev. B* **47** 16162 (1993)
218. Elias D C et al. *Science* **323** 610 (2009)
219. Ryu S et al. *Nano Lett.* **8** 4597 (2008)
220. Luo Z et al. *ACS Nano* **3** 1781 (2009)
221. Ng M L et al. *J. Phys. Chem. C* **114** 18559 (2010)
222. Lin Y, Ding F, Yakobson B I *Phys. Rev. B* **78** 041402(R) (2008)
223. Flores M Z S et al. *Nanotechnology* **20** 465704 (2009)
224. Feibelman P J *Phys. Rev. B* **77** 165419 (2008)
225. Ribas M A et al. *Nano Res.* **4** 143 (2011)
226. Cheng S-H et al. *Phys. Rev. B* **81** 205435 (2010)
227. Zbořil R et al. *Small* **6** 2885 (2010)
228. Bourlinos A B et al. *Carbon* **50** 1425 (2012)
229. Withers F, Dubois M, Savchenko A K *Phys. Rev. B* **82** 073403 (2010)
230. Robinson J T et al. *Nano Lett.* **10** 3001 (2010)
231. Jeon K-J et al. *ACS Nano* **5** 1042 (2011)
232. Chernozatonskii L A et al. *J. Phys. Chem. C* **115** 132 (2011)
233. Lebègue S et al. *Phys. Rev. B* **79** 245117 (2009)
234. Muñoz E et al. *Diamond Relat. Mater.* **19** 368 (2010)
235. Sahin H, Topsakal M, Ciraci S *Phys. Rev. B* **83** 115432 (2011)
236. Gao H et al. *J. Phys. Chem. C* **115** 3236 (2011)
237. Chandrachud P et al. *J. Phys. Condens. Matter* **22** 465502 (2010)
238. Li Y et al. *J. Phys. Chem. C* **113** 15043 (2009)
239. Samarakoon D K, Wang X-Q *ACS Nano* **3** 4017 (2009)
240. Sahin H, Ataca C, Ciraci S *Phys. Rev. B* **81** 205417 (2010)
241. Ashfold M N R et al. *Chem. Soc. Rev.* **23** 21 (1994)
242. Chernozatonskii L A et al. *JETP Lett.* **90** 134 (2009) [*Pis'ma Zh. Eksp. Teor. Fiz.* **90** 144 (2009)]
243. Samarakoon D K, Wang X-Q *ACS Nano* **4** 4126 (2010)
244. Leenaerts O, Partoens B, Peeters F M *Phys. Rev. B* **80** 245422 (2009)
245. Kita Y, Watanabe N, Fujii Y *J. Am. Chem. Soc.* **101** 3832 (1979)
246. Watanabe N *Solid State Ionics* **1** 87 (1980)
247. Touhara H et al. *Z. Anorg. Allgem. Chem.* **544** 7 (1987)
248. Kurmaev E Z et al. *Phys. Lett. A* **288** 340 (2001)
249. Chernozatonskii L A et al. *JETP Lett.* **85** 77 (2007) [*Pis'ma Zh. Eksp. Teor. Fiz.* **85** 84 (2007)]
250. Chernozatonskii L A, Sorokin P B, Brüning J W *Appl. Phys. Lett.* **91** 183103 (2007)
251. Chernozatonskii L A, Sorokin P B *Phys. Status Solidi B* **245** 2086 (2008)
252. Chernozatonskii L A, Sorokin P B *J. Phys. Chem. C* **114** 3225 (2010)
253. Ruoff R *Nature Nanotechnol.* **3** 10 (2008)
254. Singh A K, Yakobson B I *Nano Lett.* **9** 1540 (2009)
255. Openov L A, Podlivaev A I *JETP Lett.* **90** 459 (2009) [*Pis'ma Zh. Eksp. Teor. Fiz.* **90** 505 (2009)]
256. Huang L F et al. *J. Phys. Chem. C* **115** 21088 (2011)
257. Ao Z M et al. *Appl. Phys. Lett.* **97** 233109 (2010)
258. Han S S, Kim H, Park N J. *Phys. Chem. C* **115** 24696 (2011)
259. Ratnikov P V *JETP Lett.* **90** 469 (2009) [*Pis'ma Zh. Eksp. Teor. Fiz.* **90** 515 (2009)]
260. Zhou S Y et al. *Nature Mater.* **6** 770 (2007)
261. Giovannetti G et al. *Phys. Rev. B* **76** 073103 (2007)
262. Barbier M et al. *Phys. Rev. B* **77** 115446 (2008)
263. Park C-H et al. *Phys. Rev. Lett.* **101** 126804 (2008)
264. Park C-H et al. *Nano Lett.* **8** 2920 (2008)
265. Isacson A et al. *Phys. Rev. B* **77** 035423 (2008)
266. Guinea F, Katsnelson M I, Vozmediano M A H *Phys. Rev. B* **77** 075422 (2008)
267. Wehling T O et al. *Europhys. Lett.* **84** 17003 (2008)
268. Hornekær L et al. *Phys. Rev. Lett.* **96** 156104 (2006)
269. Nilsson L et al. *Carbon* **50** 2052 (2012)
270. Withers F et al. *Nano Lett.* **11** 3912 (2011)
271. Wei Z et al. *Science* **328** 1373 (2010)
272. Topsakal M, Sevinçli H, Ciraci S *Appl. Phys. Lett.* **92** 173118 (2008)
273. Sevinçli H, Topsakal M, Ciraci S *Phys. Rev. B* **78** 245402 (2008)
274. Huang B et al. *J. Am. Chem. Soc.* **131** 17919 (2009)
275. Wang B, Wang J *Phys. Rev. B* **81** 045425 (2010)
276. Geim A K *Rev. Mod. Phys.* **83** 851 (2011); *Usp. Fiz. Nauk* **181** 1284 (2011)